Volume 17, Issue 4, 172530 (1-19)

Iranian Journal of Earth Science (IJES)

https://doi.org/10.57647/j.ijes.2025.16894

Petrogenesis and tectonic implications of Neoproterozoic to Cenozoic A-type granitoids in NW Iran: Geochemical and tectonic constraints

Hamed Talebian Borojenie[1], Seyed Jamal Sheykhzakariaei[1], Rahim Dabiri[2,*], Abdollah Yazdi[3]

[1]*Department of Geology, SR.C., Islamic Azad University, Tehran, Iran.*
[2]*Department of Geology, Ma.C., Islamic Azad University, Mashhad, Iran.*
[3]*Department of Geology, Kah.C., Islamic Azad University, Kahnooj, Iran.*

[*]**Corresponding author:** rahim.dabiri@iau.ac.ir

Original Research

Received:
2024-03-09
Revised:
2024-05-13
Accepted:
2024-07-28
Published online:
2025-06-07
Published in issue:
2025-10-30

Abstract:

In the northwest of Iran, in the Sanandaj-Sirjan zone, type A granitoid masses related to the Late Neoproterozoic-Lower Cambrian (Ajab Shir rhyolites, Chaipareh, Mahneshan, Misho, Saqez and Sufi Abad), Mesozoic (south of Dehgolan, Ebrahim-Attar), Cenozoic (Harris and Takab) exist. In terms of geochemical characteristics, the granitoid rocks of Late Neoproterozoic-Lower Cambrian time show the characteristics of magmas related to volcanic arcs, which were formed due to a tectonic window (SCLM) in the final/post-pan-African orogeny stages. In other words, the magmatism of the active continental margin of Cadomin in Iran occurred after the main phase of Pan-African orogeny and simultaneously with the stretching of the continental crust in the Arabian-Nubian shield. But the granitoid rocks of the Mesozoic era (Late Triassic- Early Jurassic) were formed by Paleo Tethys subsidence. Cenozoic (Eocene) granitoid rocks were formed in a tensile environment after the collision of the Arabian and Eurasian plates. Most A-type granites are peraluminous, rich in iron and show enrichment of LREE elements compared to HREE. Also, the amount of MgO, CaO, Sr, Ba, Nb-Ta and Eu is low in them. Most of the granites of Sanandaj-Sirjan zone are located in the A1 range, but some are also located in the A2 range, which is due to metasomatism by fluids originating from the oceanic crust or slab-derived melts. All these granites were formed in a tensile environment.

Keywords: Granite type- A; Sanandaj-Sirjan Zone; SCLM; Neoproterozoic

1. Introduction

Extensive studies have been done on type-A granites. Type A granites mainly has been reported in Australia, China (North, East and South), Turkey, Brazil (South, South East), Poland, Norway (South and South West), France, Russia, Namibia, Cameroon, India, America. and Ethiopia (Advay et al., 2009).

A-type granites have been studied and investigated in different parts of Iran by different researchers (Mansouri Esfahani et al., 2010; Tahmasebi et al., 2010; Arvin et al., 2007; Shabanian et al., 2009; Moayyed and Hossainzade, 2011; Ghasempour et al., 2014; Yazdi et al., 2016; Shafaii Moghadam et al., 2020; Nazari et al., 2023; Nouri et al., 2023).

In the northwest of Iran, in the Sanandaj-Sirjan zone, there are type A granitoid masses related to the Late Neoproterozoic-Lower Cambrian periods (Ajab Shir rhyolites, Chaipareh, Ghoshchi, Mahneshan, Misho, Saqez and Sufi Abad), Mesozoic (Alvand leucogranites), south of Dehglan, Ebrahim-Attar) and Cenozoic (Haris and Takab).

In the Iranian Plateau, the Precambrian basement is divided into two basic parts. The first part which has been mapped by National Iranian Oil Company (N.I.O.C., 1959) arise in north, central, and eastern of Iran is formed of granitic and gneissic rocks. A wide range of crystallization ages from Archean to late Proterozoic is shown by Zircon dating (Haghipour, 1981; Samani et al., 1994; Ramezani and Tucker, 2003; Hassanzadeh et al., 2008; Azizi et al., 2011; Jamshidi Badr et al., 2013; Rossetti et al., 2014; Ousta et al., 2024). The second part which is cut by granitoid bodies

included metamorphic rocks of green schist facies. The basic mafic basement is more compatible with island arch's magmatic activity in the Proto-Tethys Ocean (Saki, 2010; Azizi et al., 2011; Dabiri et al., 2018; Elmi et al., 2025). However, there is no exact report of granitoid basement in northwest of Iran, but there are some exact researches in the Sanandaj-Sirjan zone (SaSZ) (Hassanzadeh et al., 2008; Shahzeidi et al., 2016; Badr et al., 2018; Shabanian et al., 2018).

Most Precambrian- early Paleozoic granites in the central and northwest Iran have U–Pb magmatic ages of 586 – 524 Ma (e.g., Sheikh Chupan granite, 551 ± 25 Ma, and Bubaktan granite, 544 ± 19 Ma (Hassanzadeh et al., 2008; Mollai et al., 2021); Khoy granite, 550 Ma (Azizi et al., 2011); Moteh complex, 596–578 Ma (Hassanzadeh et al., 2008); Soursat, 540 Ma (Jamshidi Badr et al., 2013); Misho, 547 ± 87 Ma (Shahzeidi et al., 2016); Chapedony, 545–527 Ma (Ramezani and Tucker, 2003), Biarjmand-Torud, 565–522 Ma (Moghadam et al., 2013) and Lahijan, 572–551 Ma (Hassanzadeh et al., 2008).

Middle to Upper Jurassic magmatism in the SaSZ subsequently occurred in an Andean-like tectonic setting, marked by large calcalkaline granitic intrusions at the onset of Early Jurassic subduction of the Neo-Tethys ocean underneath the SaSZ and Central Iranian microcontinent (Shahbazi et al., 2010; Mahmoudi et al., 2011; Esna-Ashari et al., 2012; Chiu et al., 2013; Davoudian et al., 2016).

Paleocene and Eocene granitoids ranging from ca. 34 to 58 Ma include Saqqez (Mahmoudi et al., 2011; Azizi et al., 2019; Ashrafi et al., 2024), Takab (Jamshidi Badr et al., 2013), Naqadeh Piranshahr (Mazhari et al., 2009a; Mazhari et al., 2009b), Gusheh-Tavandasht (Mahmoudi et al., 2011), Marivan (Sepahi et al., 2014) and Baneh (Azizi et al., 2018). Azizi et al. (2019) have suggested that magma generation resulted from a transpressional tectonic regime during early stages of the collision of Arabia and Eurasian plates during Eocene.

The northern Iran plutonic rocks, belong to the Sanandaj-Sirjan Zone (SSZ). The SSZ represents the suture zone between the Afro-Arabian and the Iranian plate which is a result of the opening and later closure of the Neotethys between Eurasia and Arabia (Berberian and King, 1981a; Mohajjel et al., 2003; Ghasemi and Talbot, 2006). The Sanandaj–Sirjan zone is characterized by deformed metamorphic rocks which are associated with numerous plutons and a widespread volcanism. The plutons cropping out in the North part of the SSZ (i.e., Qorveh, Urumieh, Alvand, Saqez, Malayer-Boroujerd) are generally formed during the Mesozoic (Torkian et al., 2008; Ghalamghash et al., 2009; Shahbazi et al., 2010; Arian et al., 2011; Deevsalar et al., 2014).

The oldest crust in NW Iran consists of Ediacaran-Early Cambrian (Cadomian) igneous and minor sedimentary rocks (Kahar Formation), covered by Cambrian sedimentary rocks (Naghizadeh, 2004). These rocks are intruded by Late Devonian, Carboniferous to Permian A-type granites and alkaline gabbronorites and are unconformably overlain by Permian sedimentary rocks. Jurassic to Early Cretaceous magmatic rocks are also present in NW Iran and are the along-strike continuation of the SaSZ.

In this article, we are going to discuss and investigate the geochemistry, genesis and origin of these rocks by comparing the type-A granites in the northwest of Iran in different times from the Neopertozoic to the Cenozoic, and finally the way of formation of this type of granites, that is, the type-A granites in the north West of Iran in the Sanandaj-Sirjan zone.

2. Geology

The study area is located in the northern part of Sanandaj-Sirjan zone (Fig. 1) and belongs to Khoy-Mahabad zone (Nabavi, 1976). Igneous, metamorphic and sedimentary rocks ranging in age from Percambrian to Quaternary present in the area (Fig. 2).

Chaypareh granitic-gabbroic intrusions are located within

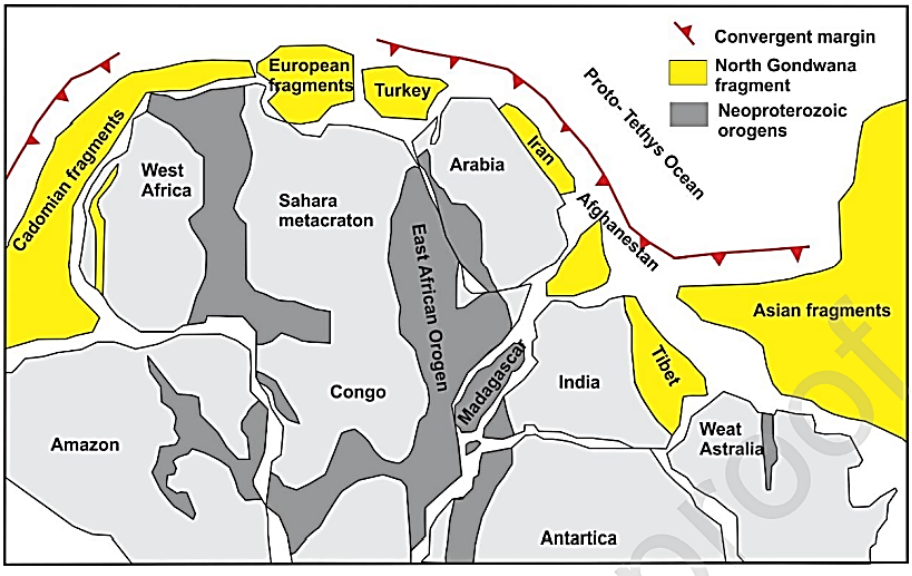

Figure 1. Map of a part of Gondwana, showing the position of continents fragments in Neoprotrozoic orogeny (Stern, 2023).

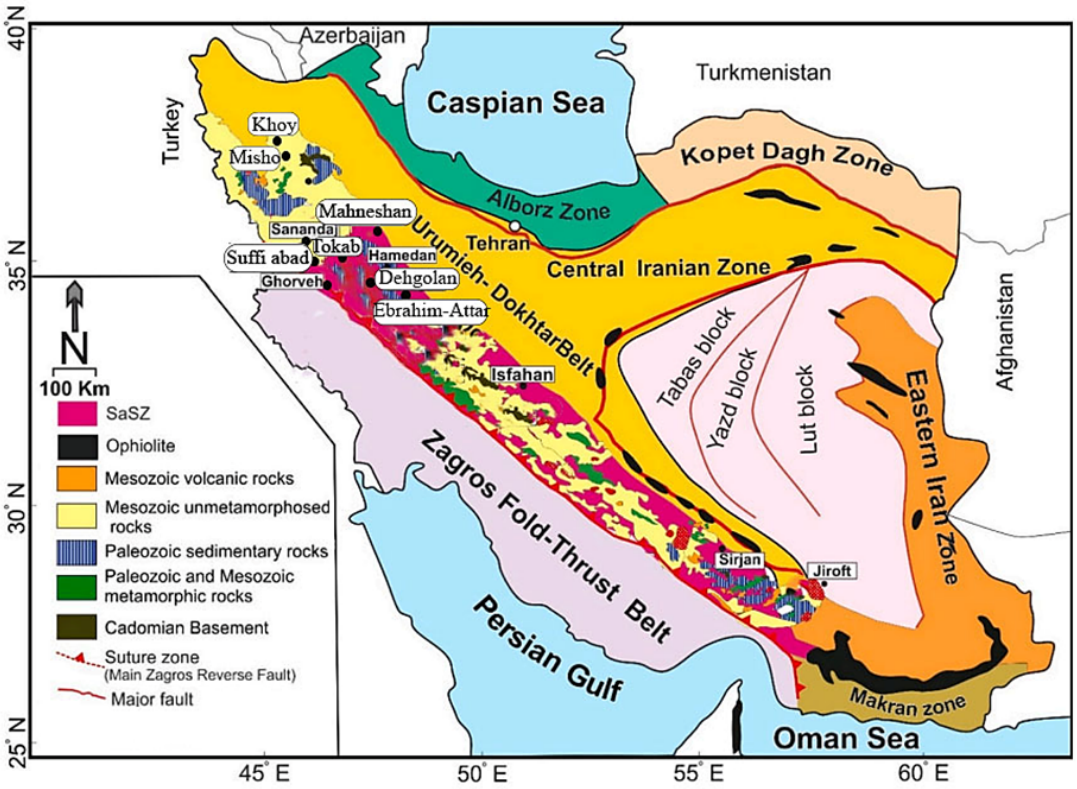

Figure 2. Simplified geological map of the Sanandaj-Sirjan Zone (SaSZ) and its Jurassic granitoid plutons in Iran (modified after Bayati et al. (2017) and Azizi et al. (2019)). In the figure above, the investigated environments are marked with red circles.

the Sanandaj-Sirjan structural zone and 35 km northwest of Khoy city (Stöcklin, 1968; Oskuie and Hajialilu, 1995; Fazlnia, 2017).

Most of the rocks in this zone are metamorphic rocks of the Mesozoic era and sedimentary rocks of the Cenozoic era (Berberian and King, 1981b; Alavi, 1994). During the opening of the Neonis in the late Carboniferous-early Permian, the Sanandaj Sirjan zone was separated from the Gondwana supercontinent (Golonka, 2004). However, in the Permian-Triassic period, this zone moved towards Eurasia, and after that, two regional transformation events occurred in a part of this zone (Fazlnia et al., 2009). At the end of the Cenozoic, after the continental collision between the Arabian and Eurasian plates, a part of the collision zone became Zagros and evolved when the Neotethys closed (Berberian and King, 1981a; Alavi, 1994; Mohajjel et al., 2003; Golonka, 2004; Mouthereau et al., 2012; Mohajjel and Fergusson, 2014). In the studied area, Precambrian metamorphic rocks and sedimentary rocks are outcropped (Oskouei and Haj Alilou, 1995). The oldest units Paleozoic rocks of the region are fine-grained and metamorphosed slate and phyllite sandstones related to the Precambrian Kahr Formation (Fig. 3). These rocks are generally crushed and tectonized. The Permian related units have a limited outcrop in the south of the Shah Ashan Dagh granite, which consists of dark red quartzite sandstones with shale interlayers along with Permian sedimentary limestones. This unit has been cut by Shah Ashan granite and metamorphic aura has been created in these rocks (Fig. 4). Studies have shown that these granites are of the same age as the Ghoshchi granites and were formed in the late Carboniferous-early Permian period (Fazlnia, 2017; Arjmandzadeh et al., 2021). In the Cretaceous rock units that are studied in the east of the granite, they have a fault boundary with the granite and include limestone and marly limestone. The Oligo-Miocene units in this region can be seen scattered and wide in the west and south of the Shah Ashan Dagh granite, which mostly include milky white fine-grained limestones and in some cases with clay interlayers. This unit with a conglomerate base containing granite fragments covers the Shah Ashan Dagh massif. Shah Ashan Dagh massif is formed from felsic and mafic rocks. The mafic rocks of the Shah Ashan Dagh massif are limited outcrops of gabbroic rocks that can be seen in the north and south of the massif. The mafic rocks in the south of the mass are cut by granitic rocks, while the mafic rocks in the north of the mass do not show any connection with the granite mass. The felsic part of the mass has a granitic composition and has a fleshy red to pale pink color which are visible among the Permian intrusion units and Mafic masses rocks (Fig. 4).

3. Analytical procesures

During field operations, 50 samples were taken in systematic sampling, of which 40 thin sections were prepared. The samples were among the fresh outcrops and the weathered rims of the samples were removed before packing in plastic sample bags. and were studied by using Zeiss polarizing microscope in the Islamic Azad University, Science and Research Branch, Tehran. We used two main analytical procedures including: 1) X-Ray Fluorescence (XRF) and

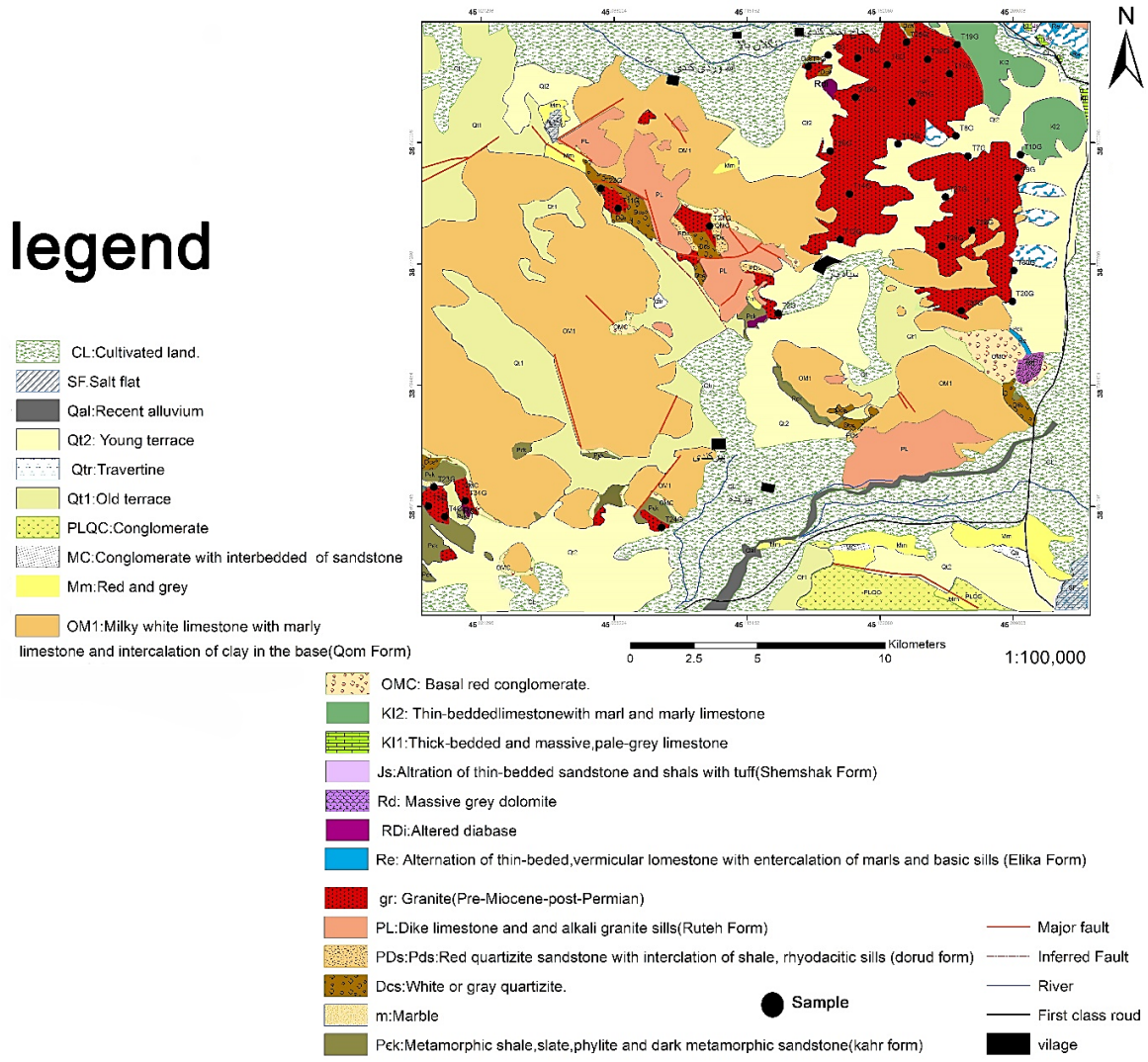

Figure 3. The geological map of the studied area along with the sampled points taken from the 1:100,000 map of Qara Ziauddin (Oskuie and Hajialilu, 1995).

Inductively Coupled Plasma-Mass Spectrometry (ICP-MS) for whole-rock major- and trace-element analyses; the We studied 17 for whole rock samples chemical analysis in Zarazma Company of Iran.

4. Lithography

The petrographic studies show that the granitoid mass of Chaipareh region is composed of acidic igneous rocks including alkali feldspar granite, granodiorite, sino-granite and monzo granite and basic igneous rocks such as diorite and gabbro. Granodiorites are the largest outcrops in terms of extent

A. Alkali feldspar granites

These stones are seen in orange or red color in the desert due to the presence of potassium feldspar, and they are widespread in the region. These rocks are mainly coarse-grained (granular texture) and consist of alkali feldspar, plagioclase and quartz. These stones are mainly coarse grain (granular texture) and consist of alkali feldspar, plagioclase and quartz. Among their secondary minerals, we can refer to opaque minerals and zircon, and from secondary minerals to sericite, iron oxide (hematite) and chlorite.

A. Sinogranite and Monzo granites

In the samples, granular texture, graphic, veined peritite can be seen (Fig. 5 a) and plagioclase crystals are often subautomorphized and sericitized. In plagioclases, Carlsbad and polysynthetic along with fluctuating zoning are observed. Among their secondary minerals, we can mention opaque minerals, and secondary minerals include sericite, iron oxide (hematite) and chlorite. The main constituent minerals, in order of abundance, usually include quartz ($30-35\%$), potassium feldspar ($20-25\%$), plagioclase ($20-25\%$) and amphibole and their secondary minerals include sphene, zircon, apatite, biotite and Opec minerals (primary and secondary).

B. Granodiorites

These stones are less widespread in the region than other types. The bright minerals of these rocks include plagioclase ($45-55\%$), quartz ($20-22\%$) and potassium feldspar ($10-18\%$) in small amount and secondary minerals include

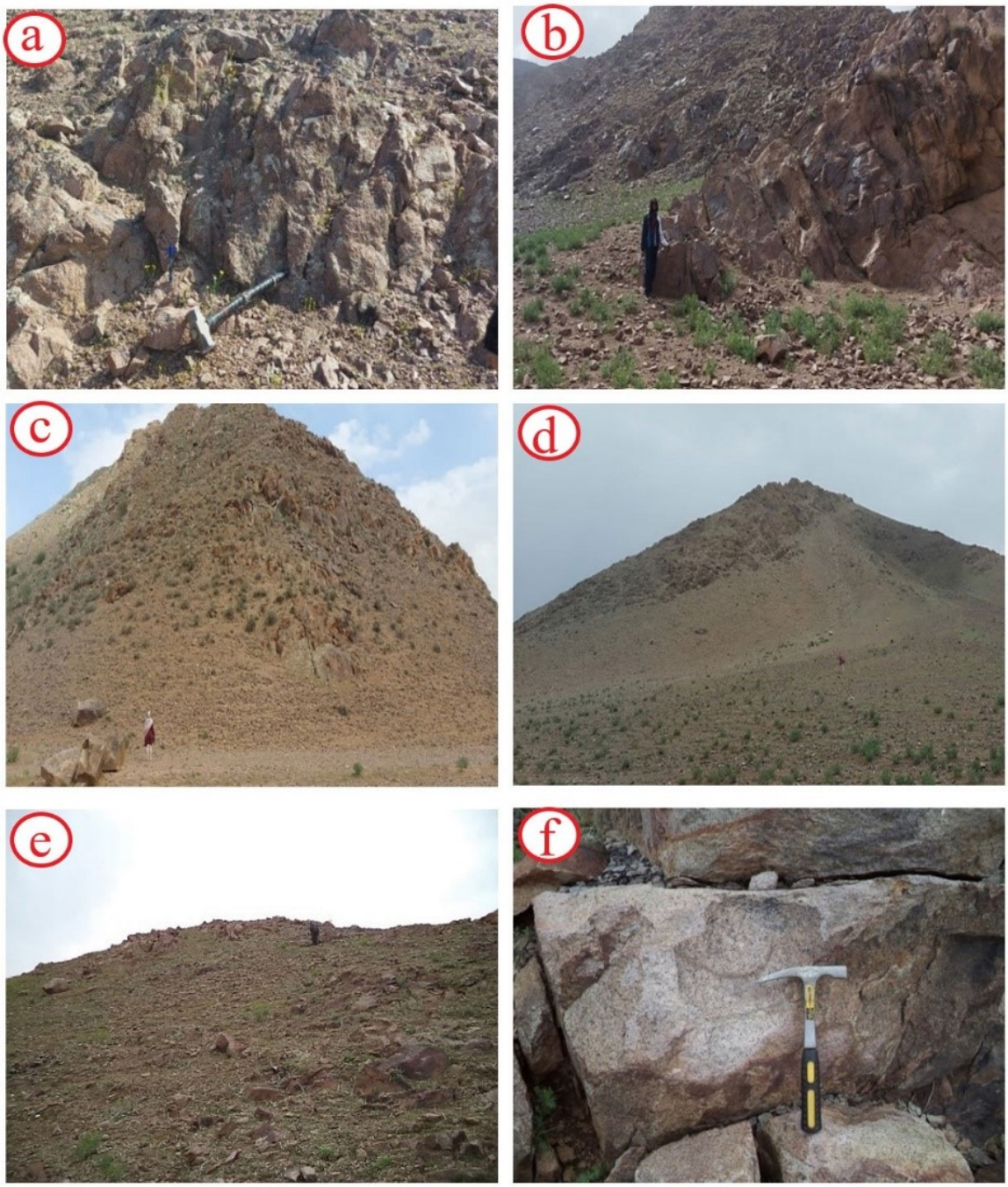

Figure 4. A- A view of the granite masse around the village of Yarim Ghiya. B-A view of Shah Ashan Dagh granite masses. C- A view of Shah Ashan Dagh granite masse around Siah Baz village, view to the north. D- A view of the granite masse in the southeast of Zanglan village, view to the north. E- A view of granite masses north of Haji Ahmed Kandi village. F- A view of the erosion of granite masses north of Haji Ahmad Kandi village.

biotite, amphibole, sphene and opac. Chlorite and sericite minerals are secondary minerals. Their microscopic texture is subhedral granular (semi-shaped grains), dynamic and graphic (Fig. 5 b).

C. Gabbros

The characteristic textures of the area are granular and micro granular. Plagioclase is present in the form of fine crystals with an average frequency of 50 to 60% in these rocks. Fine crystals are present in the form of needle-like microlites in the field of samples with porphyric texture. Quartz with an abundance of less than 10% and the space between plagioclase fills the coarse crystal minerals. Augite can be found in shaped to semi-shaped form. Apatite and sphene are secondary and important minerals found in gabbroic rocks (Fig. 5 c).

5. Geochemistry of granitic and gabbroic rocks of northwestern Iran

In order to study and investigate the geochemistry and petrogenesis of acidic and basic intrusive rocks in northwest Iran and compare the research results of different researchers in these areas we deal with granite and gabbro stones of Chaipare region.

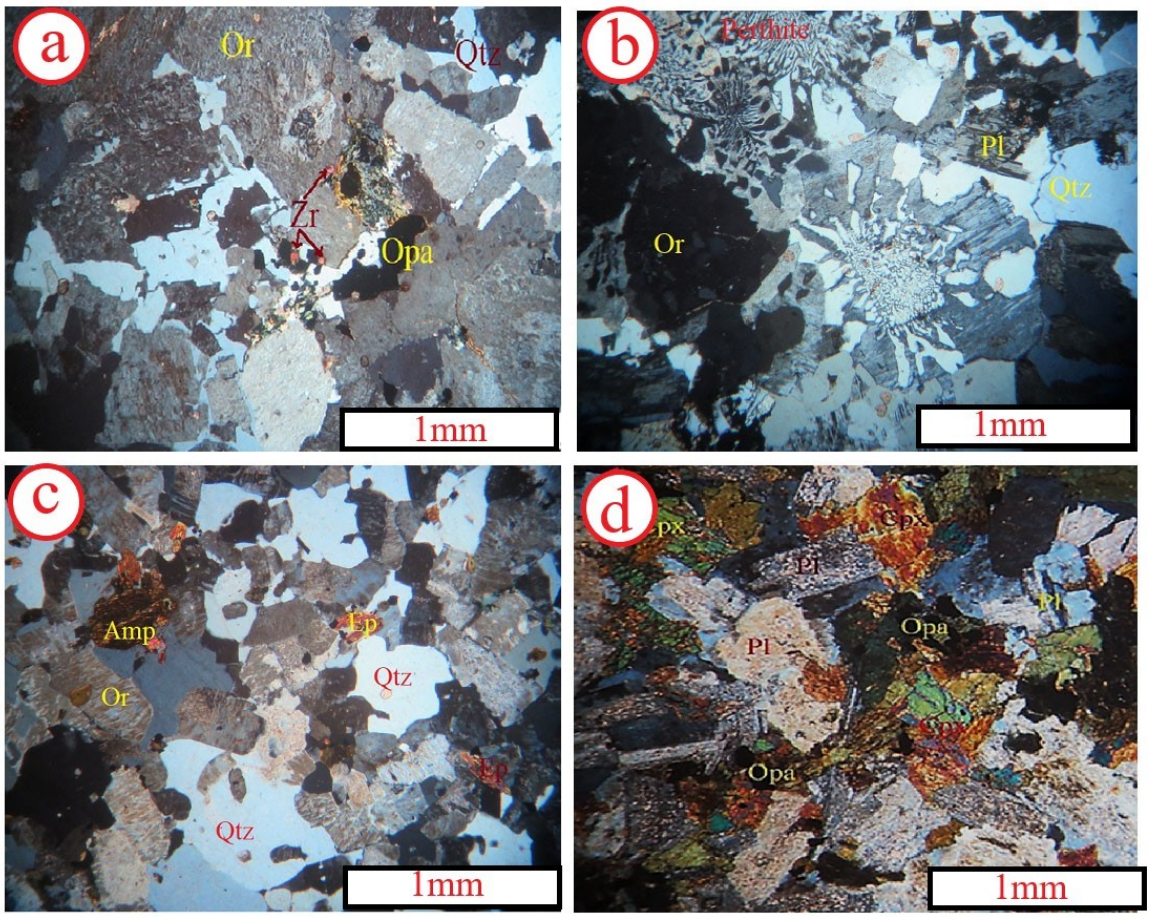

Figure 5. A- A view of perthite texture in sino granite. B- A view of the granular texture and the presence of hornblende in Monzo granite. c-granular texture and the presence of zircon and chlorite in alkali granite. d- Granular texture and the presence of plagioclase and clinopyroxene minerals in gabbro.

According to the diagram of Middlemost (1994), all samples are placed in the sub-alkaline range (Fig. 6 a, c). In the diagram ($Na_2O + K_2O - CaO$, in the opposite figure, samples are preferentially placed in the calc-alkaline and alkali-calcic fields (Frost, 2001). Aluminum saturation index [A/CNK = mol% $Al_2O_3/(CaO + Na_2O + K_2O)$] varies from 0.95 to 1.05, and A/NK > 1, also the samples are mainly meta to peraluminous(Fig. 6 b). In the FeO*/FeO* + MgO versus SiO_2 differentiation diagram from Frost (2001), the samples are placed in the combined field of A-type and Fe-rich granites (Fig. 6 d).

The amount of Al_2O_3 decreases with the increase of SiO_2, which indicates the crystallization of silicate minerals such as plasioclase and amphibole during magma crystallization (Fig. 7 a). In addition, the reduction of Eu content with the increase of SiO_2 indicates the crystallization of plagioclase (Fig. 7 c). The increase of ASI (alumina saturation index or ASI) and Zr/Hf with the increase of SiO_2 content indicates the important role of subtraction of mafic silicate minerals such as biotite and amphibole during magma crystallization (Fig. 7 f). The alkali feldspar granites of Khoy and some areas in the northwest of Iran have high FeOt and Na_2O due to having amphibole (ribkite), but they have less MgO and CaO than type I granites, which highlight their iron-rich features, type A. A-type granites have high amounts of Na_2O, K_2O, FeO, F, Zr, Nb, Rb, Ga, Y and REE except (Eu) and CaO, Sr and Ba are less. These types of granites can be divided into A1 and A2 granites. A1 type granites are per alkaline and originate from subduction of magmas sources such as OIB. While A2 granites are peraluminous and subtraction products from tholeiitic magmas and/or relatively melted products of the lower continental crust (Fig. 8). Also, the positive correlation between Sr and Ba in these rocks indicates the separation of potassium feldspar during magma crystallization. The positive correlations between Ba and Sr (Fig. 7) indicate that the parental magmas of the granites experienced K-feldspar fractionation.

However, distinguishing A-type granites from highly differentiated I-type granites is particularly difficult (Whalen et al., 1987; King et al., 1997). Based on diagrams of Na_2O vs. K_2O (Fig. 8 a) and $CaO/(FeOt + MgO + TiO_2)$ vs. $CaO + Al_2O_3$ (Dall'Agnol and Oliveira, 2007; Yanbo and Jingwen, 2010) all our analyzed samples and almost the northwest Iran granites plot within A-type fields (Fig. 5 b). The northwest Iran granites show both A1 and A2-type geochemical signatures (Fig. 9); they have high Nb/Ta and Zr/Hf ratios similar to mantle values and much lower Ce/Nb and Y/Nb ratios similar to OIBs but resembling continental crust in Nb/U ratio (Fig. 10 a, b). In the logarithmic plot of Th/Yb vs. Nb/Yb from Pearce and Peate (1995), most granite rocks of northwest Iran show subduction-related environments (Fig. 10 c).

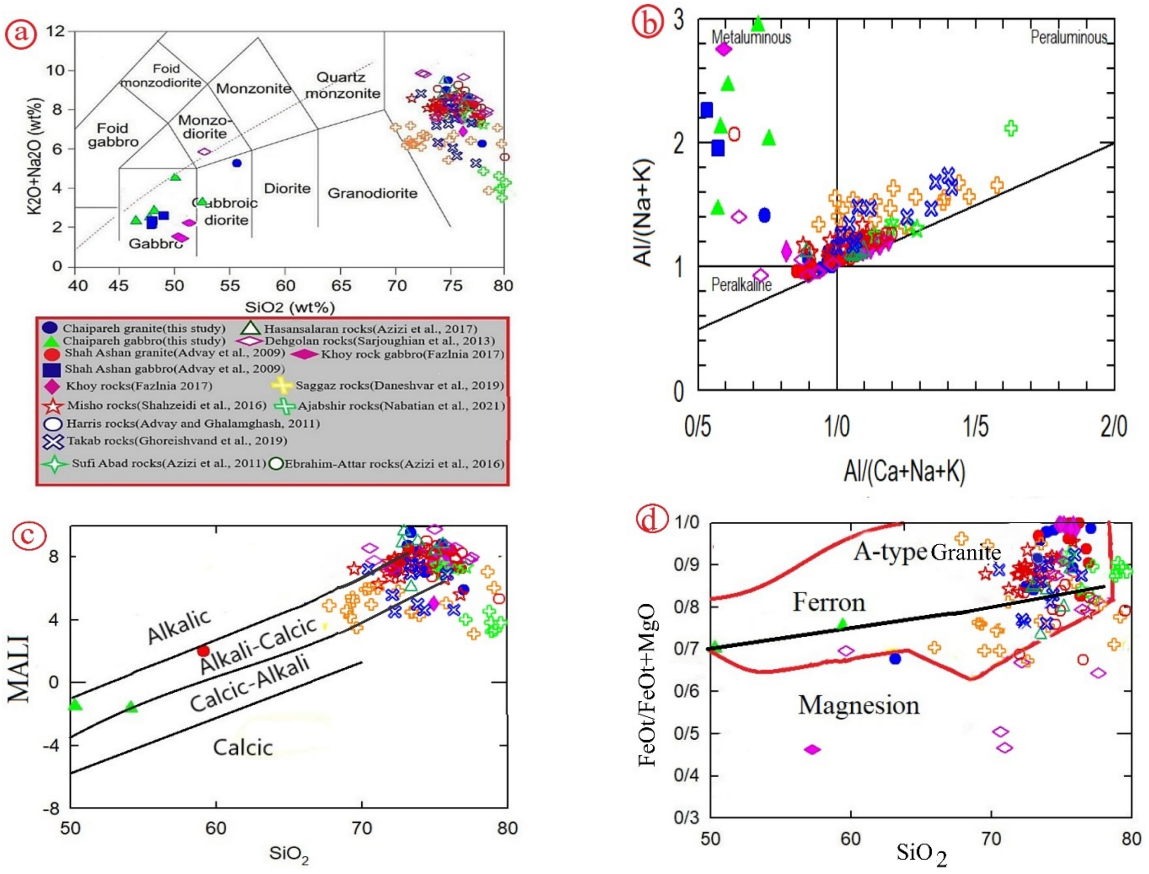

Figure 6. A- total alkalis ($Na_2O + K_2O$) vs. silica (TAS) diagram (Middlemost, 1994). B- Plots of the granite samples in a modified alkali lime index ($Na_2O + K_2O$ - CaO) vs SiO_2 discrimination diagram (Frost and Frost, 2011) showing an alkali-calcic nature. C- Molar A/CNK [Al_2O_3/ ($CaO + Na_2O + K_2O$)] vs. A/NK [(Al_2O_3)/ ($Na_2O + K_2O$)] diagram (Maniar and Piccoli, 1989). D- FeOt / (FeOt + MgO) vs. SiO_2 diagram (Frost, 2001).

In order to better study and investigate the enrichment and depletion of trace elements, we used the average of these elements in the granite rocks of different places in the northwest of Iran. In the distribution pattern of rare earth elements normalized to chondrite and primary mantle, the relative enrichment of LREES compared to HREES is visible. In the normalized spider diagram to the primary mantle for the granites of northwestern Iran, Rb shows a positive anomaly and Ba, Sr and Ti elements show a negative anomaly (Fig. 11 a). In addition, the studied granites are clearly rich in LILES elements, especially Rb and Th, but they are poor in Sr, Eu, Nb, Ti, and Ba elements, which indicate the origin of these granites from crustal melts. The rocks also show variable negative Nb-Ta anomalies, a feature likely inherited from a mantle source metasomatized by melt/fluid released from a subducting slab. On the other hand, in the investigated granites, barium accumulates well in alkali feldspars and sedic amphiboles.

But the low amount of Sr indicates the low amount of modal plagioclase feldspar (Rollinson, 1993). The low percentage of cesium also indicates that the paternal magma of these rocks was devoid of this element. In granites, Eu shows a significant negative anomaly (Fig. 10 a), since Eu is a compatible element in feldspars, especially in plagioclase), its anomaly can be the result of plagioclase crystal separation during magma crystallization or instead of feldspar remaining in the origin during Partial melting in conditions where the activity of H_2O is low (Rollinson, 1993; Tepper et al., 1993) in addition to the mentioned phenomena, the negative anomaly of Eu along with the enrichment of REE against MREE and HREE) shows the importance of the role of separation Crystalline amphibole and plagioclase are in the evolution process of granitoids (Zheng et al., 2008; Huang et al., 2008) (these features are consistent with the low amount of Sr in granites, adding to this, perhaps the source rock of granitic melts is also devoid of Eu. The obvious negative anomalies in the immobile incompatible elements with high ionic strength (or HFSE such as Hf, Ta, Nb and Sr along with element (P) indicate that the origin of the granites was either void of these elements or followed by immobilization, or remaining minerals which supporting these elements (such as rutile spinel and apatite could not enter the melt at the origin (Rollinson, 1993). Also, the positive anomaly in Ti indicates that perhaps titanite was an unstable mineral during melting in liquidus of origin (Gill, 2010; Best, 2003). The granite rocks of the region are also normalized compared to ORG (hypothetical mid-ocean ridge granite) and a decreasing trend from Rb to Yb is observed (Fig. 11 d). Depletion of Ba is also observed in this graph.

6. Tectonic setting and petrogenesis

The A-type granites are similar to both volcanic-arc and within-plate granites in plots of Rb vs Y + Nb, Rb vs Ta

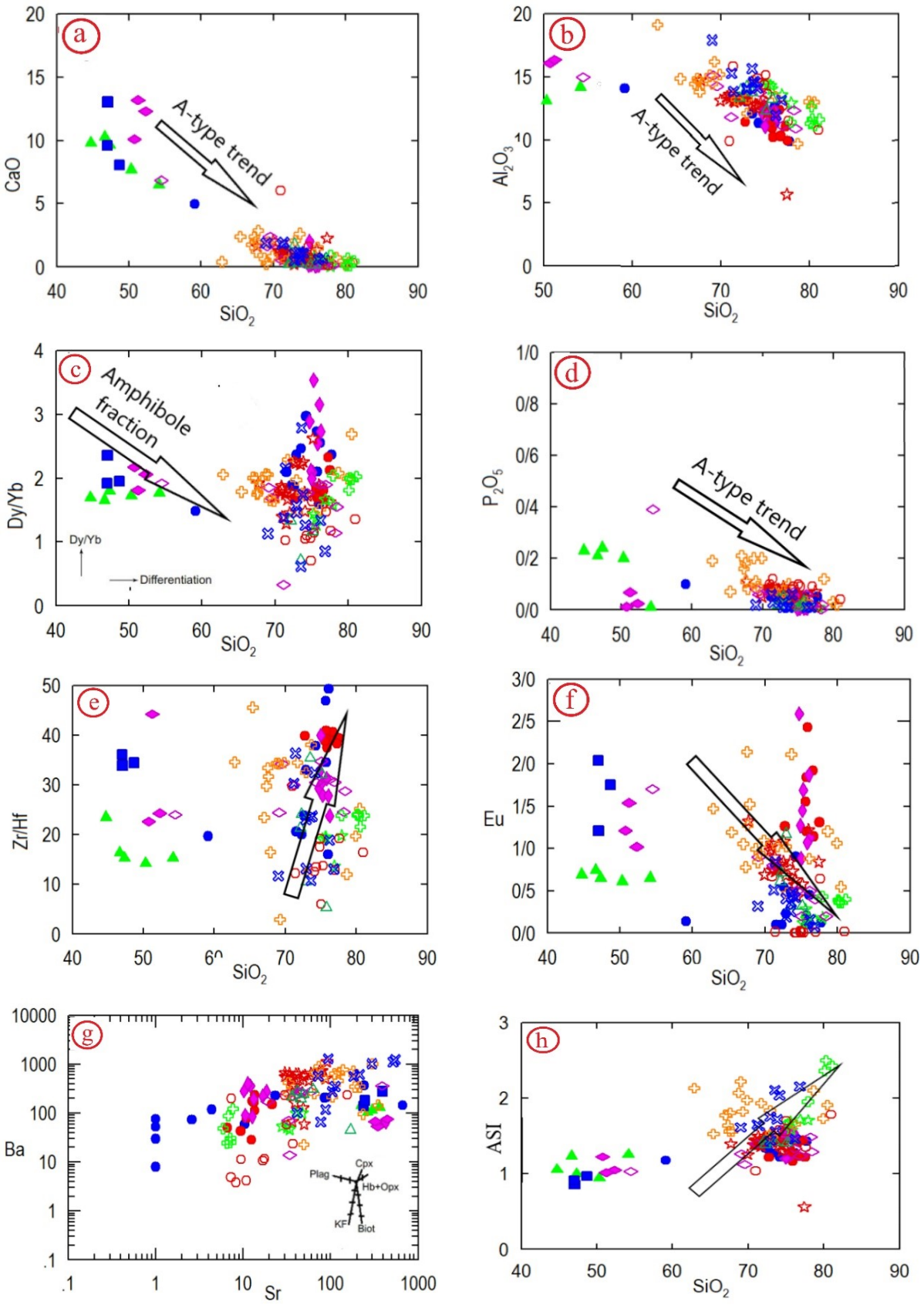

Figure 7. Variation diagrams of CaO, Al_2O_3, P_2O_5, Eu, ASI and Zr/Hf versus SiO_2 content for the northwest Iran granites. Variation diagrams of Ba versus Sr after (Yang et al., 2008).

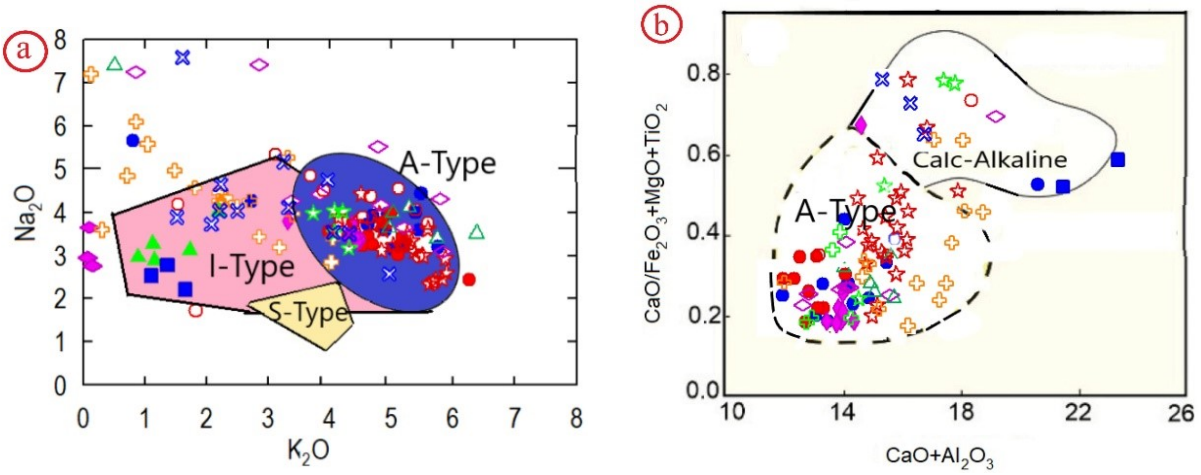

Figure 8. (a) Whole-rock Na_2O vs. K_2O (b) CaO/ (FeOt + MgO + TiO_2) vs. CaO + Al_2O_3 diagrams showing the composition of A-type granites compared with calcalkaline granites (Dall'Agnol and Oliveira, 2007; Yanbo and Jingwen, 2010).

+ Yb, Nb vs Y and Ta vs Yb (Fig. 12). On the tectonic discrimination diagram of Maniar and Piccoli (1989), the granitic rocks plot in the field of POG (Fig. 13 a), and on the tectonic discrimination diagram (Schandl and Gorton, 2002), all samples plot in the active continental margin field (Fig. 13 b). In a La vs. La/Sm plot (Blein et al. (2001); Fig. 14 a), the granite rocks show higher La/Sm ratios with increasing La contents suggesting a lower degree of partial melting, whereas the granites rocks show small variation in La/Sm ratios, suggesting fractional crystallization. In

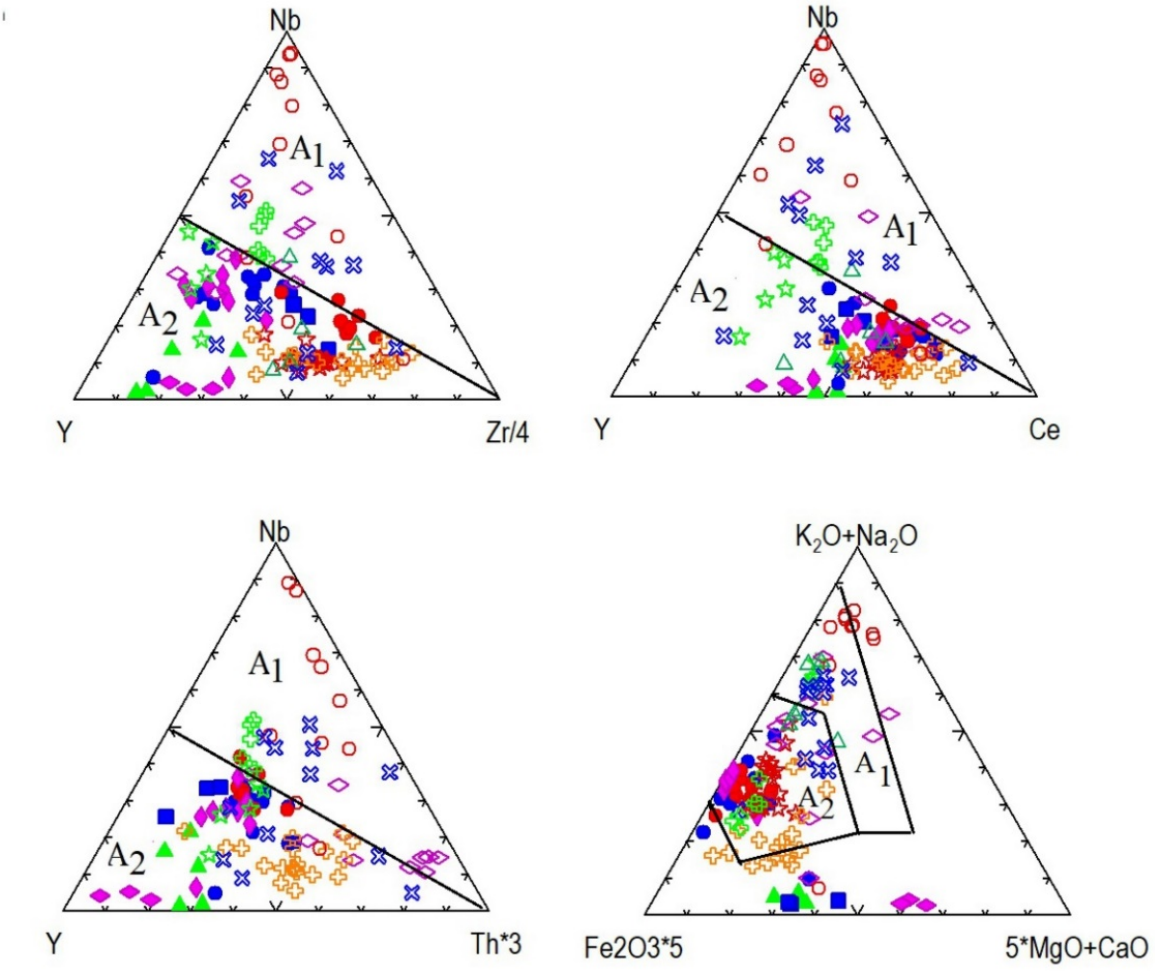

Figure 9. Nb-Y-Zr/4, B- Nb-Y-Ce, and C- Nb-Y-3*Th diagrams (Eby, 1990). D-Variations in (Na_2O + K_2O) vs Fe_2O_3 T × 5 vs. (CaO + MgO) × 5 (in molar quantities; Grebennikov (2014)).

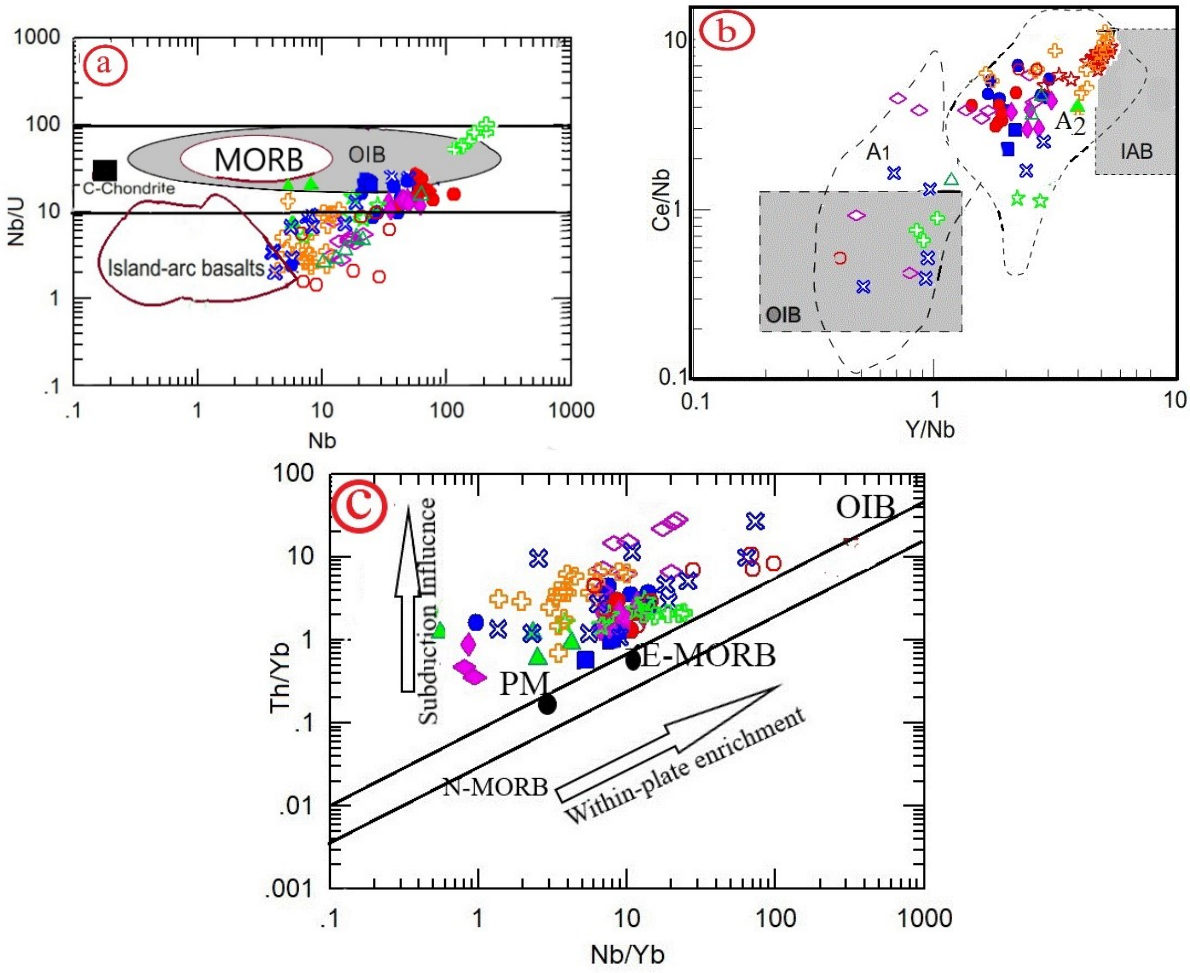

Figure 10. a-Nb/U vs Nb (Kepezhinskas et al., 1996) and b- Ce/Nb vs Y/Nb (Eby, 1992) plots for intrusive rocks from NW Iran. MORB and OIB fields in C and D panels are after Hofmann et al. (1986). C- diagram Pearce and Peate (1995).

La/Yb vs. Yb (Fan et al., 2004; He et al., 2009) and Ce/Yb vs. Ce diagrams (Ajaji et al. (1998), Fig. 14 b and c), the granites pluton shows sub-parallel trends as expected of fractional crystallization processes in melts derived from a mutual parental magma with assimilation.

Six models have been proposed to explain the formation of the A-type magmas including: (1) partial melting of an anhydrous lower crustal granulitic residue from which a granitic melt had previously been extracted (Clemens et al., 1986); (2) melting of tonalite or granodiorite in the shallow crust (Patiño Douce, 1997); (3) fractional crystallization of mantle-derived melts (Shellnutt and Zhou, 2007) and (4) mixing between basaltic and crustal melts with or without AFC processes (Collins et al., 2019). (5) variable mixtures of asthenospheric mantle and continental crust melts (Dahlquist et al., 2010); and (6) metasomatism of crustal regions by percolation of alkaline fluids released from mantle-derived magmas (Bea et al., 2001; Montero et al., 2009; Moreno et al., 2014; Moreno et al., 2016; Moreno et al., 2017). Partial melting in the stability field of plagioclase, as indicated by negative Eu, Ba and Sr anomalies of A-type granites, is considered as an important mechanism for their generation. However, the source rocks can vary from F- and Cl-enriched lower crustal granulite residues, tonalite and granodiorite at low pressures (4 kbar) and high temperatures (950 °C), and lower crustal basaltic rocks (Frost and Frost, 1997). Creaser et al. (1991) have shown that a residual granulitic source is unlikely to generate A-type granitic melts as it is too refractory.

Differential crystallization of melts derived from the mantle can be involved in the genesis of A1 granites. In this case, these granites will be associated with large sets of mafic rocks (Frost, 2001). Recent studies have shown that type-A granites can be created as a result of the subduction of an active and young interoceanic ridge under the continental crust and as a result of the function of the ridge-pit model and the creation of a lithospheric window setting (Slab window setting). Such tectonic sites have been reported in the Central Asian Orogenic Belt (CAOB) from China to the Caucasus, and in them, in addition to A-type granites, rocks with other diverse compositions such as OIB and tholeiite, adakitic rocks and normal arc rocks are formed (Király et al., 2020; Windley and Xiao, 2018) In addition, in recent studies, the existence of a ridge-pit tectonic situation and the formation of a lithospheric window in the northeast of Turkey and in the south of the Black Sea have also been reported.

Fractional crystallization of mantle-derived melts might be ruled out for generating A-type granitoids in NW Iran because these granites are not associated with contemporary

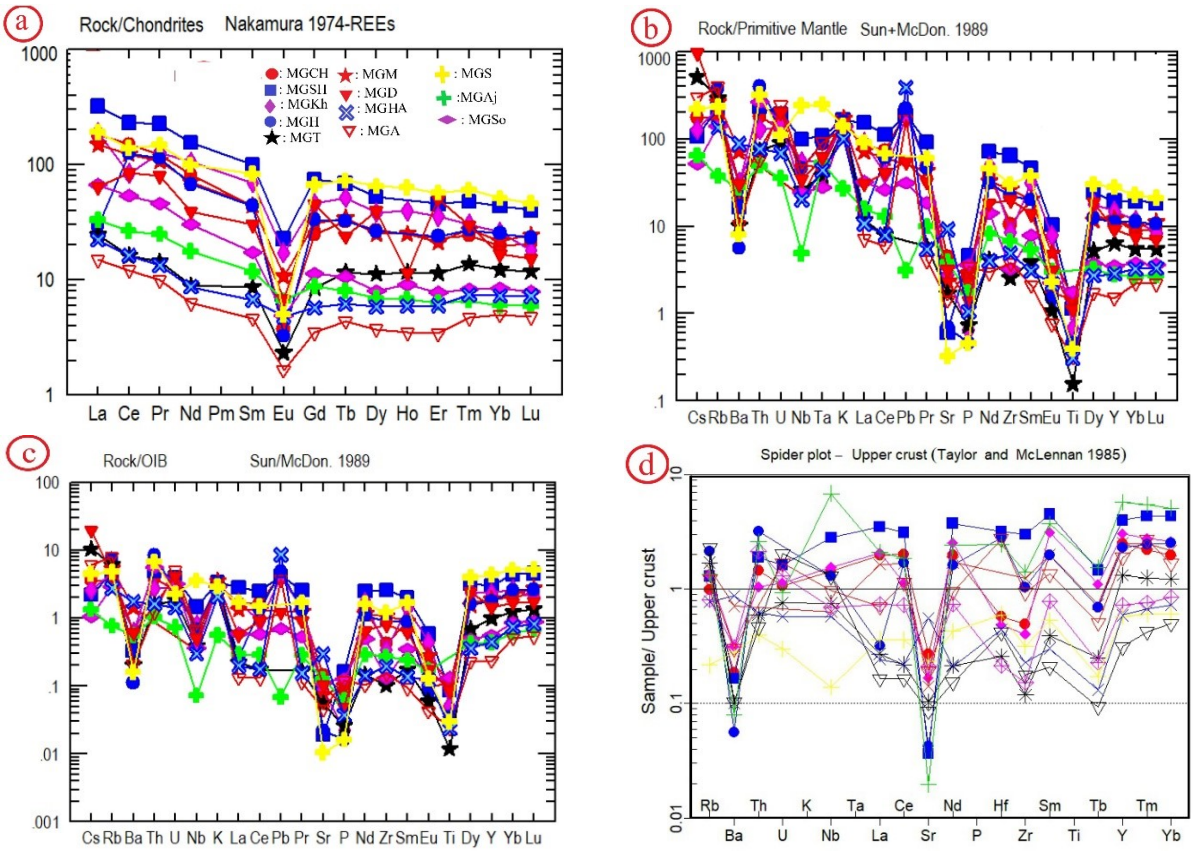

Figure 11. The average of rare earth elements of northwest Iran granites in the normalized spider diagrams A- Chondrite. B- Primary mantle. c- OIB from Sun and McDonough (1989). d- ORG from Pearce et al. (1984). Average of Misho granites- MGD; Average of Dehgolan granites- MGH: Average of Harris granites- MGT: Average of Takab granites- MGSo: Average of Sufi Abad granites- MGMa: Average of Mah Nishan granites- MGS: Average of Saqez granites- MGA: Average of Ibrahim- Attar granites - MGAj: average rhyolites of Ajab Shir.

mafic or intermediate igneous rocks. The possibility of simple fractional crystallization is supported by (1) reasonable fractionation trends in major and trace element abundances within the rock suite (Fig. 6 and 13); (2) a strong similarity of REE patterns and incompatible element ratios between the gabbro and quartz-monzodiorite (Soesoo, 1997). Somewhat similar, linear trends of chemical elements can be produced by magma mixing of, for instance, mantle derived and crustal magmas. Magma mixing is an attractive hypothesis to explain chemical variations in igneous rocks, particularly in granites. Unfortunately this term is sometimes misused in literature. Here, the term 'mixing' refers to any combination of two or more components, such as liquids and crystals, or liquid and liquid and crystals etc. Strictly speaking, most geological processes involving melts and temperature gradients are a subject of mixing. For example, melt generation through partial melting is likely to be a combination of continued mixing of small melt pockets. This is the case for fractional crystallization where only an ideal case of crystal fractionation may preserve the strict boundaries between crystallized phases and melt (and even that may not be valid when only a small percentage of melt is left) (Soesoo, 2000).

In the (Fig. 15 a) Rb/Ba has been plotted against Ti/Y. Simple mixing of mantle- and crustal-derived magmas will lead to curved mixing arrays on such a plot. However most of A-type granitoids in NW Iran plot as a cluster which is characteristic feature of fractionation. A similar topology is obtained when plotting Rb/Ba v. Th/Nb (not shown). Incompatible trace element ratios are robust during early and intermediate stages of fractionation and should not change much on type of plots like Nb/Zr v. Nb (Fig. 15 b). The scatter of Nb/Zr ratios of A-type granitoids in NW Iran is larger within the particular rock type than between the different rock types suggesting that the chemistry of these rocks may have mainly been controlled by fractionation instead of differences in partial melting of source rock or mixing processes (Soesoo, 2000).

According to the graphs in figure 10 and 12, which show the majority of granites in the northwest of Iran, the process of subtractive crystallization, that is, the third model presented for the formation of granites. But the main origin and the way of their formation, or in other words, the geodynamics of this part of Iran, i.e. Sanandaj-Sirjan zone, will be discussed in the following. Most of the granites in northwestern Iran are found along with gabbroic, diorite and monzo gabbroic rocks with OIB or ophiolitic complexes characteristics, which can be mentioned as gabbro Khoi, Harris gabbro, Khoi ophiolite, Dehglan gabbro, Misho gabbro. Of course, in some regions, such as the moon, signs of metamorphism or transformation are also observed in the rocks of the region. All these evidences indicate the formation of a lithospheric window (slab window setting) (Fig. 16).

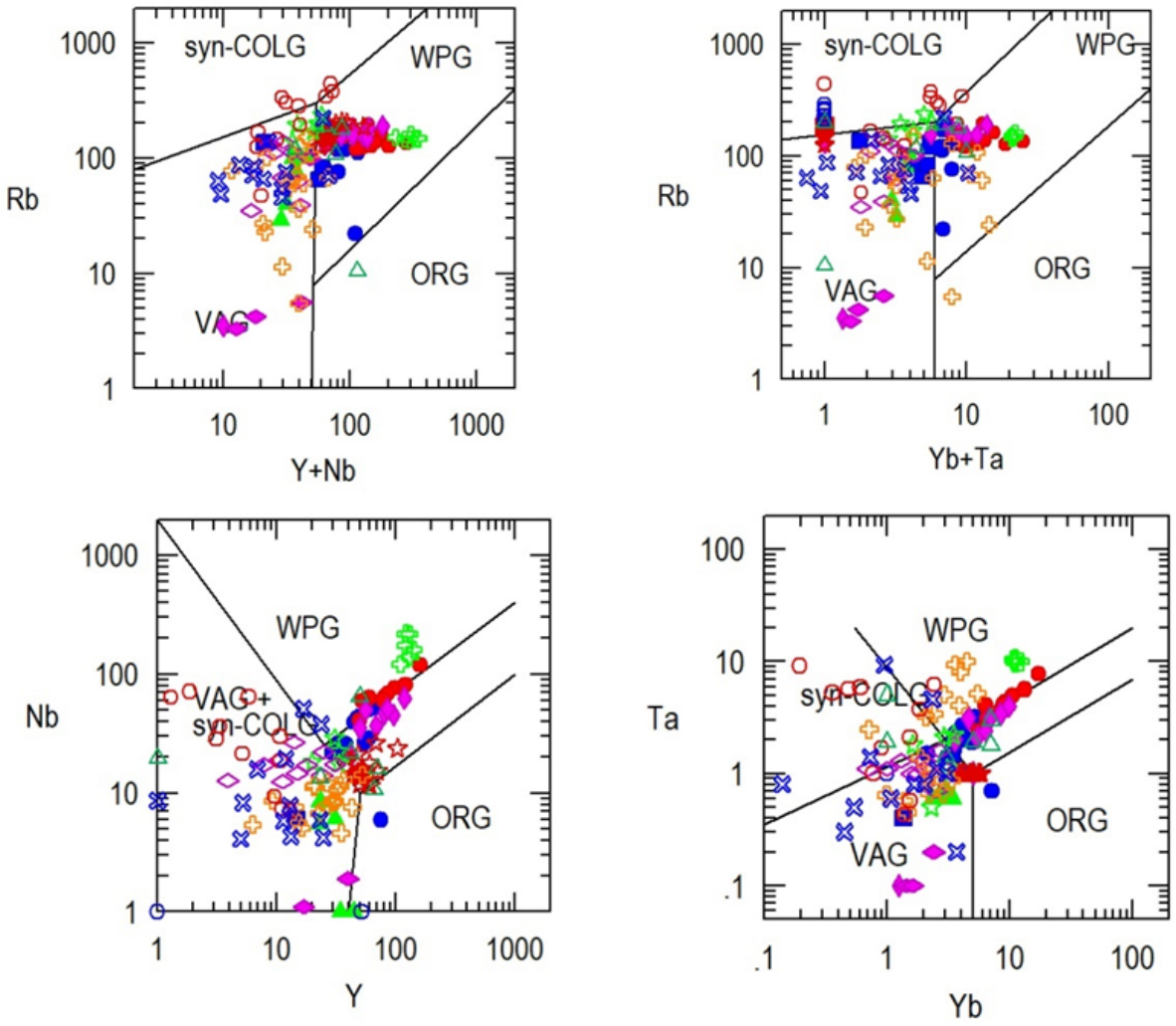

Figure 12. Diagrams (Pearce et al., 1984) for classification of granites from NW Iran.

7. Geodynamic

Subduction-related magmatic arcs produce huge accumulations of felsic to intermediate calc-alkaline igneous rocks and are considered the main constitutes of new continental crust on Earth (Ducea et al., 2015). In contrast, continental lithospheric rifting introduces bimodal magmatism through the production of a large volume of tholeiitic mafic bodies, abundance of S-type granites and some A-type granites (Zhang et al., 2018; Azizi et al., 2019).

In order to better investigate the geodynamics of the granite rocks in northwestern Iran, geodynamic developments are investigated in three time periods: 1- the end of the Carboniferous, 2- the end of the Cretaceous, and 3- the

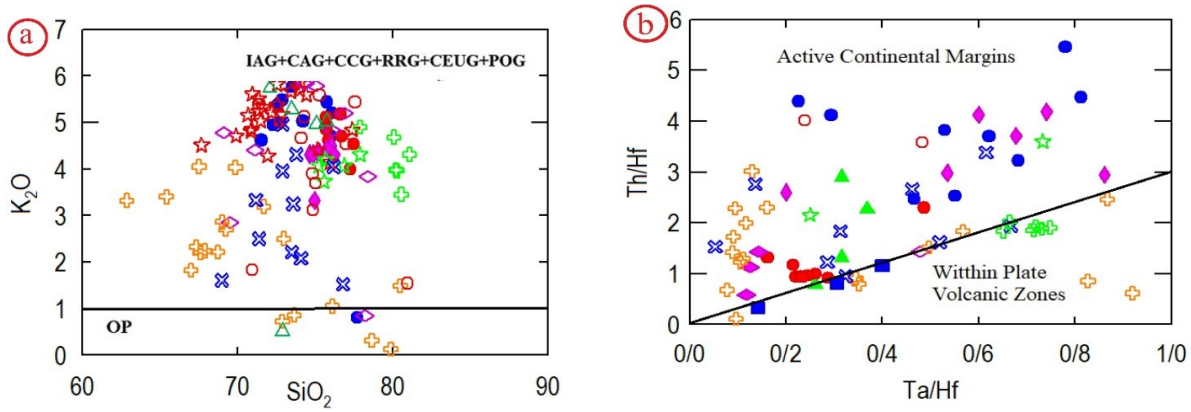

Figure 13. a-Tectonic discriminant diagram (Maniar and Piccoli, 1989) for the studied granites. The granites plot in the POG: b- in tectonic discriminant diagram (Schandl and Gorton, 2002), all samples plot in active continental margin fieled.

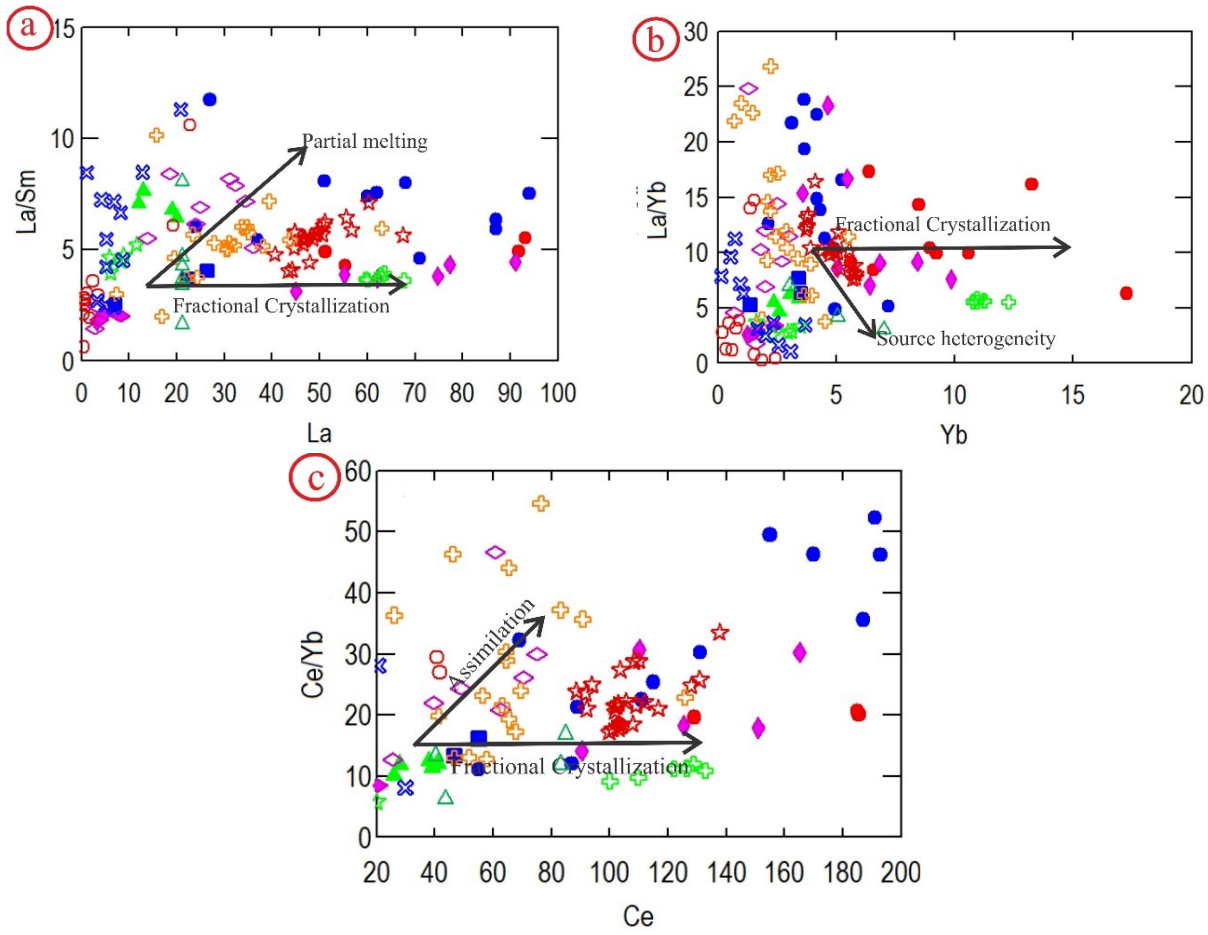

Figure 14. A- La vs La/Sm diagram (Blein et al., 2001), (B) La/Yb vs. Yb (Fan et al., 2004), and (C) Ce/Yb vs. Ce (Ajaji et al., 1998) diagrams showing trends of fractional crystallization with assimilation for the rocks (except for granites).

beginning of the Paleocene.

A. Magmatic changes at the end of the Carboniferous

Paleotethys subsidence under Central Iran took place at the end of the Carboniferous. This hot and young subducted oceanic slab was separated by transform faults, then a small tectonic window was formed under the Sanandaj-Sirjan zone. The hot asthenospheric mantle beneath the slab ascended through the created tectonic window and a gap filled with asthenosphere between the subducting and diverging oceanic plates in response to the subduction of the ridge, as a result of partial melting of this asthenospheric mantle,

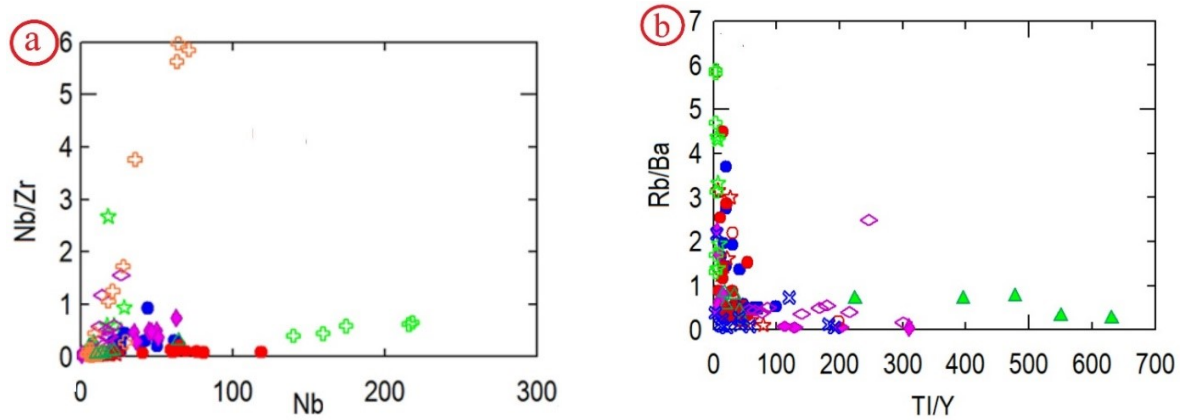

Figure 15. a- Nb versus Nb/Zr plot of A-type granitoids in NW Iran. Since the Nb/Zr ratio is immune to the effects of alteration and fractionation, it should not change much if these rock groups are the results of fractional crystallization. Mixing of distinct magmas and differences in source melting will produce inclined arrays. b- Ti/Y versus Rb/Ba plot of A-type granitoids in NW Iran. Note that A-type granitoids in NW Iran mostly form a cluster which is characteristic for suites derived from fractional crystallization of a common parental magma. Mixing will lead to curved mixing arrays, which are not observed in this plot.

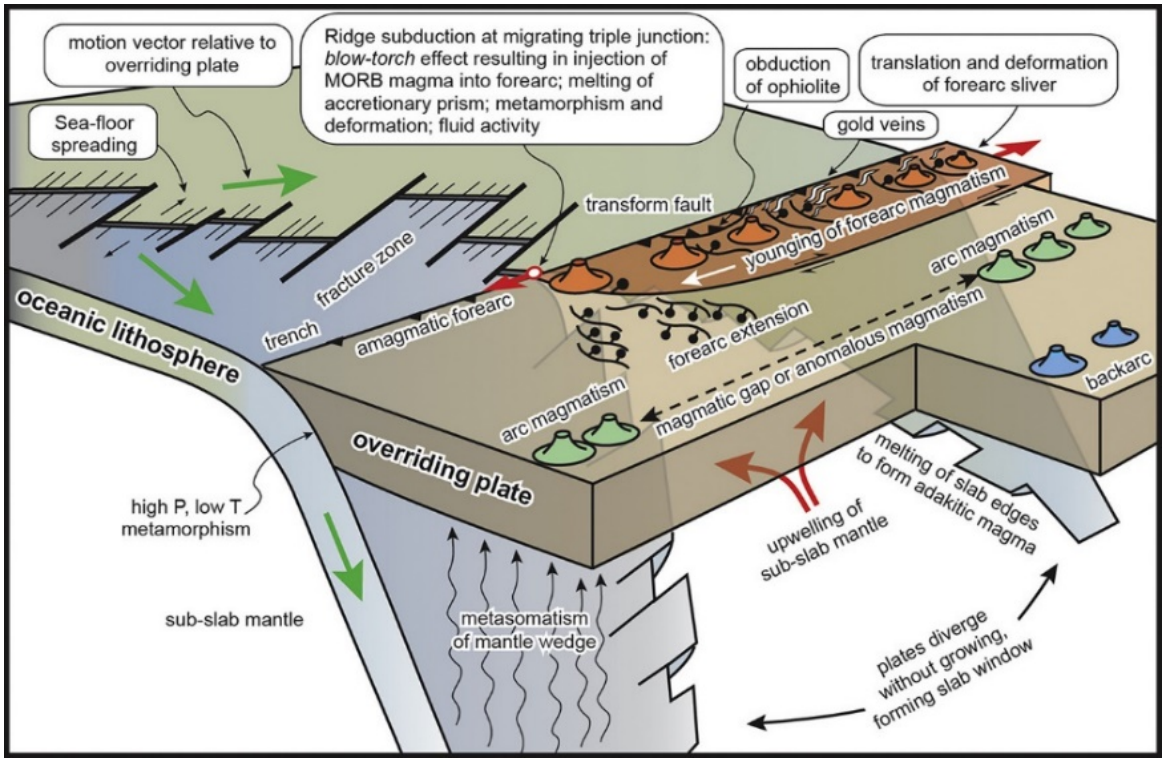

Figure 16. Triple-junction interactions with emphasis on the subduction of a migrating ridge. (Modified after Sisson and Pavlis (1993), Thorkelson (1996), and Li et al. (2015)).

OIB type gabbros have been created. At the same time, the rise of the asthenosphere created a thermal anomaly in the mantle wedge, which caused the metasomatized sub-mantle lithosphere (SCLM) and produced magmas that created the studied type A1 granites in Chaipareh and Khoi region.

B. Late Cretaceous-Early Jurassic magmatic evolutions

In the Late Cretaceous-Early Jurassic, the subduction of the Neotethys oceanic lithosphere has led to magmatic activities in the north-west of Iran. Among the A-type granites, we can mention Alvand granites (Shahbazi et al., 2010) and southern Dehglan granites (Azizi et al., 2016) and etc.
The UDMB (Urumieh-Dokhtar Magmatic Belt) defines the magmatic front (MF) associated with Neotethyan subduction. Magmatic rocks are also abundant north of the UDMB, which reflects a broad rear-arc (RA) magmatic belt. The development of a Late Cretaceous extensional regime in the UDMB and its RA regions was related to upwelling of asthenosphere above a subduction zone following subduction initiation in Late Cretaceous time. The resulting extension stimulated bimodal magmatism and allowed the formation of I-type granites and gabbro-diorites. Two models have been proposed to explain Late Cretaceous extension in Iran: (a) slab roll-back and (b) slab break-off. Slab break-off is most likely to have occurred after the collision between Iran and Arabia (Barber et al., 2018), although others argue it occurred in the Late Cretaceous (Mohajjel and Fergusson, 2000). Slab roll-back can be related to the Late Cretaceous subduction initiation (SI) (Moghadam et al., 2020). Protracted subduction initiation-related extension during the Late Cretaceous further led to continental rifting and back-arc opening across Iran. Late Cretaceous volcanic rocks are interbedded with deep water deposits above Late Cretaceous back-arc basin ophiolites such as the Sabzevar-Torbat-e-Heydarieh (STH) back-arc basin in NE and/ or Khoy in the NW. Late Cretaceous submarine volcanic sediments are also present in NNW Iran, in N Tabriz and E-SE Ardabil (Fig. 1). These volcano-sedimentary rocks are associated with Late Cretaceous deep water limestones, implying deposition in a subsiding extensional basin. Late Cretaceous calc-alkaline basalts and andesites are also abundant in the northern SaSZ, NE of Marivan (Azizi and Jahangiri, 2008) (Fig. 1 a), and are genetically related to Middle-Late Cretaceous SI. Late Cretaceous RA igneous activity is also documented for NE Iran, in the outboard RA (Kazemi et al., 2019) and in the southern UDMB (Hosseini et al., 2017) and are linked to continental rifting due to SI.

C. Paleocene magmatic evolutions

Paleocene granites type A- were emplaced in the north west of Iran $\sim$ 30 m.y. after the emplacement of the granites Type-I and gabbro-diorites. In Iran the Paleocene saw a magmatic lull, which is may be related to flat-slab subduction (Berberian and King, 1981a), that is associated with compression on the overlying plate. Also, subduction of an oceanic ridge perhaps is the result of the Paleocene magmatic lull (Agard et al., 2007) and/or seamounts (Bonnet et al., 2019). The lull was associated with compression as indicated with ophiolite exhumation in Iran, conglomerates' production controlled by ophiolite fragments along the MZT (the Amiran Formation). Current syntheses arcs in all over the world, consist of the Andes, recommend that after the subduction of the ridge or seamount; until the slab-pull force is restored, a period of slow subduction with a

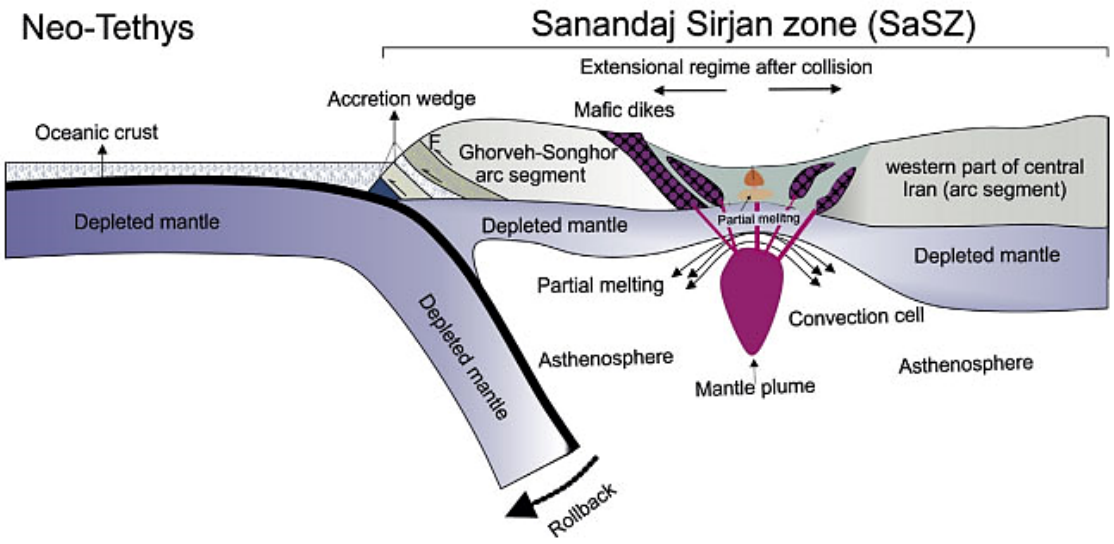

Figure 17. Schematic model for development of the EBAT SP granite Early Cretaceous (Aptian-Albian). The rollback activities of the Neo-Tethys ocean crust likely had a major role in the asthenosphere upwelling and extensional regime over the subduction zone in the northern SaSZ. During this process the thinning of the continental lithosphere occurred and temperature increasing played a major role in the partial melting of the supracrustal material (**Azizi2016**).

magmatic lull occurred e.g., (Paz et al., 2019).
In contrast, asthenospheric upwelling during the Paleocene provided heat for melting and interaction with SCLM to generate the precursor melts to the A-type granites. Subducting an actively spreading ridge often causes a "slab window" along the edges of the divergent slab. Upwelling of asthenosphere through the slab window could cause partial melting of the overlying SCLM to generate A-type granites.

8. Conclusion

Granitoid rocks in northwestern Iran are mainly meta to peraluminous and rich in iron. Investigating the geochemical characteristics of granitoid rocks in northwest Iran such as (high amount of SiO_2 (67.36-81.11 wt%), low amount of MgO (0.03-3.66 wt%), CaO (0.92-5.14 wt%), TiO_2 (0.03-2.43), low ratio of Zr/Hf (average = 26) compared to chondrite (36.44), enrichment of light REEs elements compared to heavy REEs (La/Yb = 4.20-40) is indicating A-type granite nature for granitoid rocks in the northwest Iran especially the areas around Chaipare. Analysis of spider and geotectonic diagrams showed that these granites were formed in subduction-related environments. In our opinion, the granites of northwest of Iran were formed as a result of the process of subtractive crystallization from the magma from the mantle and in three periods, the end of the Carboniferous, the end of the Cretaceous, and the beginning of the Paleocene in tensile environments as a result of subduction. Although melts from the mantle have played a major role, the contribution of the continental crust cannot be ignored. Compared to other granites of Mah Nishan, Misho, Saqez and Sufi Abad in Sanandaj-Sirjan zone, Chaipareh granites do not show any special difference in terms of geochemistry and formation environment.

Authors contributions
Authors have contributed equally in preparing and writing the manuscript.

Availability of data and materials
The data that support the findings of this study are available from the corresponding author, upon reasonable request.

Conflict of interests
The authors declare that they have no known competing financial interests or personal relationships that could have appeared to influence the work reported in this paper.

References

Advay M., Jahangiri A., Mojtahedi M., Ghalamghash J. (2009) Petrology and geochemistry of Shah Ashan Dagh mafic rocks and A-type granite in NE of Khoy, NW Iran. *Scientific Quarterly Journal, Geosciences, Islamic Republic of Iran* 20:83–90. in Persian

Agard P., Jolivet L., Vrielynck B., Burov E., Monie P. (2007) Plate acceleration: the obduction trigger?. *Earth and Planetary Science Letters* 258:428–441. DOI: https://doi.org/10.1016/j.epsl.2007.04.002.

Ajaji T., Weis D., Giret A., Bouabdellah M. (1998) Coeval potassic and sodic calc-alkaline series in the post-collisional Hercynian Tanncherfi intrusive complex, northeastern Morocco: geochemical, isotopic and geochronological evidence. *Lithos* 45:371–393.

Alavi M. (1994) Tectonic of the Zagros orogenic belt of Iran: new data and interpretations. *Tectonophysics* 229:211–238.

Arian M., Maleki Z., Noroozpour H. (2011) Cenozoic Diastrophism and Deformational Events in the East Central Alborz. *Journal of Basic and Applied Scientific Research* 1 (11): 2394–2400.

Arjmandzadeh R., Sharifi Teshnizi E., Ahmadi A. A., mahdavi A., Tavsoli S., Dabiri R. (2021) The mineralogy, geochemistry and genesis of Aghol-Messi sedimentary copper - uranium deposit, Tabas block, Central Iran. *Researches in Earth Sciences* 11 (4): 47–70. DOI: https://doi.org/10.52547/esrj.11.4.47.

Arvin M., Pan Y., Dargahi S., Malekizadeh A., Babaei A. (2007) Petrochemistry of the Siah-Kuh granitoid stock southwest of Kerman, Iran: implications for initiation of Neotethys subduction. *Journal of Asian Earth Sciences* 30:474–489. DOI: https://doi.org/10.1016/j.jseaes.2007.01.001.

Ashrafi N., Dabiri R., Jahangiri A. (2024) Some chemical variations in biotite, phlogopite, and muscovite, considering their tectonic setting. *Geopersia* 14 (2): 307–332. DOI: https://doi.org/10.22059/geope.2024.373882.648749.

Azizi H., Asahara Y., Mehrabi B., Chung S. L. (2011) Geochronological and geochemical constraints on the petrogenesis of high-K granite from the Suffiabad area, Sanandaj-Sirjan zone, NW Iran. *Chemie der Erde-Geochemistry* 71:363–376. DOI: https://doi.org/10.1016/j.chemer.2011.06.005.

Azizi H., Jahangiri A. (2008) Cretaceous subduction-related volcanism in the northern Sanandaj–Sirjan Zone, Iran. *Journal of Geodynamics* 45:178–190. DOI: https://doi.org/10.1016/j.jog.2007.11.001.

Azizi H., Lucci F., Stern R. J., Hasannejad S., Asahara Y. (2018) The late Jurassic Panjeh submarine volcano in the northern Sanandaj-Sirjan Zone, Northwest Iran: Mantle plume or active margin?. *Lithos* 308:364–380. DOI: https://doi.org/10.1016/j.lithos.2018.03.019.

Azizi H., Stern R. J., Topuz G., Asahara Y., Moghadam H. S. (2019) Late Paleocene adakitic granitoid from NW Iran and comparison with adakites in the NE Turkey: Adakitic melt generation in normal continental crust. *Lithos* 346:105151. DOI: https://doi.org/10.1016/j.lithos.2019.105151.

Azizi R., Safari A., Vaziri-Moghaddam H., Mossadegh H. (2016) Introduction of Three species of Omphalocyclus from Tarbur Formation in Semirom section (southwest of Isfahan) by comparison of Morphometric data of this genus in the Tethys area. *New Findings of Applied Geology (Bu–Ali Sina University of Hamedan, Iran)* 10:105–115.

Badr A., Davoudian A. R., Shabanian N., Azizi H., Asahara Y., Neubauer F., Dong Y., Yamamoto K. (2018) A-and I-type metagranites from the North Shahrekord Metamorphic Complex, Iran: evidence for Early Paleozoic post-collisional magmatism. *Lithos* 300:6–104. DOI: https://doi.org/10.1016/j.lithos.2017.12.008.

Barber D. E., Stockli D. F., Horton B. K., Koshnaw R. I. (2018) Cenozoic exhumation and foreland basin evolution of the Zagros orogen during the Arabia-Eurasia collision, western Iran. *Tectonics* 37:4396–4420. DOI: https://doi.org/10.1029/2018TC005328.

Bayati M., Esmaeily D., Maghdour-Mashhour R., Li H., Stern R. J. (2017) Geochemistry and petrogenesis of Kolah-Ghazi granitoids of Iran: Insights into the Jurassic Sanandaj-Sirjan magmatic arc. *Chemie der Erde-Geochemistry* 77 (2): 281–302. DOI: https://doi.org/10.1016/j.chemer.2017.02.003.

Bea F., Arzamastsev A., Montero P., Arzamastseva L. (2001) Anomalous alkaline rocks of Soustov, Kola: evidence of mantle-derived metasomatic fluids affecting crustal materials. *Contributions to Mineralogy and Petrology* 140 (5): 554–566. DOI: https://doi.org/10.1007/s004100000211.

Berberian M., King G. C. P. (1981a) Towards a Paleogeography and Tectonic Evolution of Iran. *Canadian Journal of Earth Sciences* 18:210–265.

——— (1981b) Towardsa Paleogeography and Tectonic Evolution of Iran. *Canadian Journal of Earth Sciences* 18:210–265.

Best M. G. (2003) Igneous and Metamorphic Petrology. *2nd edition, Blackwell, England*

Blein O., Lapierre H., Schweickert R. A. (2001) A Permian island-arc with a continental basement: the Black Dyke Formation Nevada, North American Cordillera. *Chemical Geology* 175:543–566.

Bonnet G., Agard P., Angiboust S., Fournier M., Omrani J. (2019) No large earthquakes in fully exposed subducted seamount. *Geology* 47:407–410. DOI: https://doi.org/10.1130/G45564.1.

Chiu H. Y., Chung S. L., Zarrinkoub M. H., Mohammadi S. S., Khatib M. M., Iizuka Y. (2013) Zircon U-Pb age constraints from Iran on the magmatic evolution related to Neotethyan subduction and Zagros orogeny. *Lithos* 162:70–87. DOI: https://doi.org/10.1016/j.lithos.2013.01.006.

Clemens J., Holloway J. R., White A. (1986) Origin of an A-type granite; experimental constraints. *American Mineralogist* 71:317–324.

Collins W. J., Huang H. Q., Bowden P., Kemp A. T. I. (2019) Repeated S-I-A-Type Granite Trilogy in the Lachlan Orogen, and Geochemical Contrasts With A-Type Granites in Nigeria: Implications for Petrogenesis and Tectonic Discrimination. *Geological Society, London, Special Publications* 491

Creaser R. A., Price R. C., Wormald R. J. (1991) A-type granites revisited - assessment of a residual-source model. *Geology* 19:163–166.

Dabiri R., Akbari-Mogaddam M., Ghaffari M. (2018) Geochemical evolution and petrogenesis of the Eocene Kashmar granitoid rocks, NE Iran: Implications for fractional crystallization and crustal contamination processes. *Iranian Journal of Earth Sciences* 10 (1): 68–77.

Dahlquist J., Alasino P., Eby N., Galindo C., Casquet C. (2010) Fault controlled Carboniferous A-type magmatism in the proto-Andean foreland (Sierras Pampeanas, Argentina): Geochemical constraints and petrogenesis. *Lithos* 115 (1-4): 65–81.

Dall'Agnol R., Oliveira D. C. de (2007) Oxidized, magnetite-series, rapakivi-type granites of Carajás, Brazil: implications for classification and petrogenesis of A-type granites. *Lithos* 93:215–233.

Davoudian A. R., Genser J., Neubauer F., Shabanian N. (2016) 40Ar/39Ar mineral ages of eclogites from North Shahrekord in the Sanandaj-Sirjan Zone, Iran: implications for the tectonic evolution of Zagros orogen. *Gondwana Research* 37:216–240. DOI: https://doi.org/10.1016/j.gr.2016.05.013.

Deevsalar R., Ghorbani M. R., Ghaderi M., Ahmadian J., Murata M., Ozawa H. (2014) Geochemistry and petrogenesis of arc-related to intraplate mafic magmatism from the Malayer-Boroujerd plutonic complex, northern Sanandaj-Sirjan magmatic zone, Iran. *Neues Jahrbuch für Geologie und Paläontologie* 274:81–120.

Ducea M. N., Saleeby J. B., Bergantz G. (2015) The architecture, chemistry, and evolution of continental magmatic arcs. *Annual Review of Earth and Planetary Sciences* 43:299–331. DOI: https://doi.org/10.1146/annurev-earth-060614-105049.

Eby G. N. (1990) Chemical Subdivision of the A-Type Granitoids: Petrogenetic and Tectonic Implications. *Geology* 20:641–644.

——— (1992) Chemical subdivision of the A-type granitoids: petrogenetic and tectonic implications. *Geology* 20:641–644.

Elmi R., Arian M. A., Ashja Ardalan A., Yazdi A. (2025) Petrology of volcanism in the Alasht-Haraz road of the Alborz mountain range, south of Amol (north of Iran). *Iranian Journal of Earth Sciences* 17 (3) DOI: https://doi.org/10.57647/j.ijes.2025.16800.

Esna-Ashari A., Tiepolo M., Valizadeh M. V., Hassanzadeh J., Sepahi A. A. (2012) Geochemistry and zircon U-Pb geochronology of Aligoodarz granitoid complex, Sanandaj-Sirjan zone, Iran. *Journal of Asian Earth Sciences* 43 (1): 11–22. DOI: https://doi.org/10.1016/j.jseaes.2011.09.001.

Fan W. M., Guo F., Wang Y. J., Zhang M. (2004) Late Mesozoic volcanism in the northern Huaiyang tectono-magmatic belt, central China: partial melts from a lithospheric mantle with subducted continental crust relicts beneath the Dabie orogen?. *Chemical Geology* 209:27–48.

Fazlnia A. (2017) Tectonomagmatic setting of the Siahbaz A-type granitoids and mafic intrusions (Northwest of Khoy). *Petrology,* no. 30, DOI: https://doi.org/10.22108/ijp.2017.81971.

Fazlnia A., Schenk V., Straaten F. Van der, Mirmohammadi M. (2009) Petrology, geochemistry, and geochronology of trondhjemites from the Qori Complex, Neyriz, Iran. *Lithos* 112 (3–4): 413–433. DOI: https://doi.org/10.1016/j.lithos.2009.03.047.

Frost C. D. (2001) A geochemical classification for granitic rocks. *Journal of Petrology* 42 (11): 2033–2048. DOI: https://doi.org/10.1093/petrology/42.11.2033.

Frost C. D., Frost B. R. (2011) On Ferroan (A-type) granitoids: their compositional variability and modes of origin. *Journal of Petrology* 52 (1): 39–53. DOI: https://doi.org/10.1093/petrology/egq070.

——— (1997) Reduced rapakivi-type granites: the tholeiite connection. *Geology* 25:647–650.

Ghalamghash J., Mirnejad H., Rashid H. (2009) Mixing and mingling of mafic and felsic magmas along the Neo-Tethys continental margin, Sanandaj-Sirjan Zone, NW Iran: A case study from the Alvand pluton. *Neues Jahrbuch für Mineralogie-Abhandlungen: Journal of Mineralogy and Geochemistry* 186 (1): 79–93. DOI: https://doi.org/10.1127/0077-7757/2009/0133.

Ghasemi A., Talbot C. J. (2006) A new tectonic scenario for the Sanandaj–Sirjan Zone (Iran). *Journal of Asian Earth Sciences* 26:68.

Ghasempour M. R., Ghazi J. M., Biabangard H., Dabiri R. (2014) Petrogenic significance of the Plio-Quaternary Nehbandan mafic lavas, Eastern Iran. *Iranian Journal of Earth Sciences* 6:133–141.

Gill R. (2010) Igneous rocks and processes: A practical guide. *1st edition. Wiley-Blackwell, Malaysia*

Golonka J. (2004) Plate tectonic evolution of the southern margin of Eurasia in the Mesozoic and Cenozoic. *Tectonophysics* 381:235–273.

Grebennikov A. V. (2014) A-type granites and related rocks: petrogenesis and classification. *Russian Geology and Geophysics* 55 (11): 1353–1366. DOI: https://doi.org/10.1016/j.rgg.2014.10.011.

Haghipour A. (1981) Precambrian in central Iran: lithostratigraphy, structural history and petrology. *Iranian Petroleum Institute Bulletin* 81:1–17.

Hassanzadeh J., Stockli D. F., Horton B. K., Axen G. J., Stockli L. D., Grove M., Schmitt A. K., Walker J. D. (2008) U-Pb zircon geochronology of late Neoproterozoic-Early Cambrian granitoids in Iran: implications for paleogeography, magmatism, and exhumation history of Iranian basement. *Tectonophysics* 451 (1–4): 71–96.

He Y., Zhao G., Sun M., Han Y. (2009) Petrogenesis and tectonic setting of volcanic rocks in the Xiaoshan and Waifangshan areas along the southern margin of the North China Craton: constraints from bulk-rock geochemistry and Sr–Nd isotopic composition. *Lithos* 114:186–199. DOI: https://doi.org/10.1016/j.lithos.2009.08.008.

Hofmann A. W., Jochum K., Seufert M., White W. M. (1986) Nb and Pb in oceanic basalts: new constraints on mantle evolution. *Earth and Planetary Science Letters* 79:33–45.

Hosseini M. R., Hassanzadeh J., Alirezaei S., Sun W., Li C. Y. (2017) Age revision of the Neotethyan arc migration into the southeast Urumieh-Dokhtar belt of Iran: geochemistry and U–Pb zircon geochronology. *Lithos* 284:296–30. DOI: https://doi.org/10.1016/j.lithos.2017.03.012.

Huang X. L., Xu Y. G., Li X. H., Li W. X., Lan J. B., Zhang H. H., Liu Y. S., et al. (2008) Petrogenesis and tectonic implications of Neoproterozoic, highly fractionated A-type granites from Mianning, South China. *Precambrian Research* 165:190–204. DOI: https://doi.org/10.1016/j.precamres.2008.06.010.

Jamshidi Badr M., Collins A. S., Masoudi F. (2013) The U-Pb age, geochemistry and tectonic significance of granitoids in the Soursat Complex, Northwest Iran. *Turkish Journal of Earth Sciences* 22 (1): 1–31.

Kazemi Z., Ghasemi H., Tilhac R., Griffin W., Moghadam H. S., O'Reilly S., Mousivand F. (2019) Late Cretaceous subduction-related magmatism on the southern edge of Sabzevar basin, NE Iran. *Journal of the Geological Society* 176 (3): 530–552. DOI: https://doi.org/10.1144/jgs2018-076.

Kepezhinskas P., Defant M. J., Drummond M. S. (1996) Progressive enrichment of island arc mantle by melt-peridotite interaction inferred from Kamchatka xenoliths. *Geochimica et Cosmochimica Acta* 60:1217–1229.

King P. L., White A. J. R., Chappell B. W., Allen C. M. (1997) Characterization and origin of aluminous A-type granites from the Lachlan Fold Belt, southeastern Australia. *Journal of Petrology* 38 (3): 371–391. DOI: https://doi.org/10.1093/petroj/38.3.371.

Király Á., Portner D. E., Hayniede K. L., Chilson-Park B. H., Ghosh T., Jadamecdh M., Makushkina A., Mangaj M., Moresi L., O'Farrell K. A. (2020) The effect of slab gaps on subduction dynamics and mantle upwelling. *Tectonophysics* 785:228–458. DOI: https://doi.org/10.1016/j.tecto.2020.228458.

Li N. B., Niu H. C., Shan Q., Yang W. B. (2015) Two episodes of Late Paleozoic A-type magmatism in the Qunjisayi area, western Tianshan: Petrogenesis and tectonic implications. *Journal of Asian Earth Sciences* 113 (1): 238–253.

Mahmoudi S., Corfu F., Masoudi F., Mehrabi B., Mohajjel M. (2011) U-Pb dating and emplacement history of granitoid plutons in the northern Sanandaj-Sirjan Zone, Iran. *Journal of Asian Earth Sciences* 41:238–249.

Maniar P. D., Piccoli P. M. (1989) Tectonic discrimination of granitoids. *Geological Society of America Bulletin* 101 (5): 635–643.

Mansouri Esfahani M., Khalili M., Kochhar N., Gupta L. N. (2010) A-type granite of the Hasan Robat area (NW of Isfahan, Iran) and its tectonic significance. *Journal of Asian Earth Sciences* 37:207–218.

Mazhari S. A., Amini S., Ghalamghash J., Bea F. (2009a) Petrogenesis of granitic unit of Naqadeh complex, Sanandaj-Sirjan Zone, NW Iran. *Arabian Journal of Geosciences* 4:59–67.

Mazhari S. A., Bea F., Amini S., Ghalamghash J., Molina J. F., Montero P., Scarrow J. H., Williams I. S. (2009b) The Eocene bimodal Piranshahr massif of the Sanandaj-Sirjan Zone, NW Iran: a marker of the end of the collision in the Zagros orogen. *Journal of the Geological Society, London* 166:53–69. DOI: https://doi.org/10.1144/0016-76492008-022.

Middlemost E. A. (1994) Naming materials in the magma/igneous rock system. *Journal of Asian Earth Sciences* 37:215–224.

Moayyed M., Hossainzade G. (2011) Petrology and petroghraphy of A-type Granitoides of the East-Misho Mountain with theory on its geodynamic importance. *Journal of Mineral Crystal* 3:529–544.

Moghadam H. S., Li Q. L., Li X. H., Stern R. J., Levresse G., Santos J. F., Lopez Martinez M., Ducea M. N. G., et al. (2020) Neotethyan Subduction Ignited the Iran Arc and Backarc Differently. *Journal of Geophysical Research (solid Earth)* 125 DOI: https://doi.org/10.1029/2019JB018460.

Moghadam H. S., Stern R. J., Chiaradia M., Rahgoshay M. (2013) Geochemistry and tectonic evolution of the Late Cretaceous Gogher–Baft ophiolite, central Iran. *Lithos* 168:33–47.

Mohajjel M., Fergusson C. L. (2000) Dextral transpression in late cretaceous continental collision, Sanandaj-Sirjan Zone, western Iran. *Journal of Structural Geology* 22:1125–1139.

——— (2014) Jurassic to Cenozoic tectonics of the Zagros Orogen in northwestern Iran. *International Geology Review* 56:263–287.

Mohajjel M., Fergusson C. L., Sahandi M. R. (2003) Cretaceous-Tertiary convergence and continental collision, Sanandaj-Sirjan zone, Western Iran. *Journal of Asian Earth Sciences* 21:397–412.

Mollai H., Dabiri R., Torshizian H. A., Pe-Piper G., Wang W. (2021) Upper Neoproterozoic garnet-bearing granites in the Zeber-Kuh region from east central Iran micro plate: Implications for the magmatic evolution in the northern margin of Gondwanaland. *Geologica Carpathica* 72 (6): 461–481. DOI: https://doi.org/10.31577/GeolCarp.72.6.2.

Montero P., Bea F., Corretgé L. G., Floor P., Whitehouse M. J. (2009) U-Pb ion microprobe dating and Sr and Nd isotope geology of the Galineiro igneous complex: a model for the peraluminous/peralkaline duality of the Cambro-Ordovician magmatism of Iberia. *Lithos* 107 (3–4): 227–238. DOI: https://doi.org/10.1016/j.lithos.2008.10.009.

Moreno J. A., Baldim M. R., Semprich J., Oliveira E. P., Verma S. K., Teixeira W. (2017) Geochronological and geochemical evidences for extension-related Neoarchean granitoids in the southern São Francisco Craton, Brazil. *Precambrian Research* 294:322–343. DOI: https://doi.org/10.1016/j.precamres.2017.04.011.

Moreno J. A., Molina J. F., Bea F., Anbar M. A., Montero P. (2016) Th-REE-and Nb-Ta accessory minerals in post-collisional Ediacaran felsic rocks from the Katerina Ring Complex (S. Sinai, Egypt): an assessment for the fractionation of Y/Nb, Th/Nb, La/Nb and Ce/Pb in highly evolved A-type granites. *Lithos* 258:173–196. DOI: https://doi.org/10.1016/j.lithos.2016.04.020.

Moreno J. A., Molina J. F., Montero P., Anbar M. A., Scarrow J. H., Cambeses A., Bea F. (2014) Unraveling sources of A-type magmas in juvenile continental crust: constraints from compositionally diverse Ediacaran post-collisional granitoids in the Katerina Ring Complex, southern Sinai, Egypt. *Lithos* 192:56–85. DOI: https://doi.org/10.1016/j.lithos.2014.01.010.

Mouthereau F., Lacombe O., Vergés J. (2012) Building the Zagros collisional orogen: Timing, strain distribution and the dynamics of Arabia/Eurasia plate convergence. *Tectonophysics* 532–535:27–60.

Nabavi M. H. (1976) An introduction to the Iranian geology. *Geological Survey of Iran, Tehran,* in Persian

Naghizadeh R. (2004) 1/100000 Geological Map of Oshnavieh. *Geological Survey and Mineral Exploration of Iran, Tehran*

Nazari M., Arian M. A., Solgi A., Zarei sahamieh R., Yazdi A. (2023) Geochemistry and tectonomagmatic environment of Eocene volcanic rocks in the Southeastern region of Abhar, NW Iran. *Iranian Journal of Earth Sciences* 15 (4): 228–247. DOI: https://doi.org/10.30495/ijes.2023.1956689.1746.

N.I.O.C. (1959) Geological Map of Iran, 1:2,500,000. *National Iranian Oil Company*

Nouri F., Azizi H., Asahara Y., Stern R. (2023) A new perspective on Cenozoic calc-alkaline and shoshonitic volcanic rocks, eastern Saveh (central Iran). *International Geology Review* 63 DOI: https://doi.org/10.1080/00206814.2020.1718005.

Oskouei A., Haj Alilou B. (1995) Geological map of the Qara Zia al-Din quadrangle, Geological Organization of Iran.

Oskuie A., Hajialilu B. B. (1995) Explanatory text of Qara-Ziaaddin. *Geological Quadrangle Map 1:100000, No. 5067. Geological Survey of Iran, Tehran*

Ousta S. H., Ashja-Ardalan A., Yazdi A., Dabiri R., Arian M. A. (2024) Petrogenesis and tectonic implications of Miocene dikes in the southeast of Bam (SE Iran): Constraints on the development of active continental margin. *Geopersia* 14 (1): 89–111. DOI: https://doi.org/10.22059/geope.2023.364334.648729.

Patiño Douce A. E. (1997) Generation of metaluminous A-type granites by low-pressure melting of calc-alkaline granitoids. *Geology* 25:743–746.

Paz L. F., Bechis F., Litvak V. D., Echaurren A., Encinas A., González J., Lucassen F., Oliveros V., Valencia V., Folguera A. (2019) Constraints on Trenchward Arc Migration and Backarc Magmatism in the North Patagonian Andes in the Context of Nazca Plate Rollback. *Tectonics* 38 (11): 3794–3817. DOI: https://doi.org/10.1029/2019TC005580.

Pearce J. A., Harris N. B., Tindle A. G. (1984) Trace element discrimination diagrams for the tectonic interpretation of granitic rocks. *Journal of Petrology* 25 (4): 956–983.

Pearce J. A., Peate D. W. (1995) Tectonic implications of the composition of volcanic arc magmas. *Annual Review of Earth and Planetary Sciences* 23:251–285.

Ramezani J., Tucker R. D. (2003) The Saghand region, Central Iran: U-Pb geochronology, petrogenesis and implications for Gondwana tectonics. *American Journal of Science* 303 (7): 622–665.

Rollinson H. R. (1993) Using geochemical data: evaluation, presentation, interpretation. *1st edition, Longman Scientific and Technical, London*

Rossetti F., Nasrabady M., Theye T., Gerdes A., Monié P., Lucci F., Vignaroli G. (2014) Adakite differentiation and emplacement in a subduction channel: the late Paleocene Sabzevar magmatism (NE Iran). *Geological Society of America Bulletin* 126 (3–4): 317–343.

Saki A. (2010) Proto-Tethyan remnants in northwest Iran: geochemistry of the gneisses and metapelitic rocks. *Gondwana Research* 17 (4): 704–714. DOI: https://doi.org/10.1130/B30913.1.

Samani B. A., Zhuyi G., Xuetao G., Chuan T. (1994) Geology of Precambrian in central Iran; On the context of stratigraphy, magmatism and metamorphism. *Geosciences Quarterly* 3 (10): 40–63.

Schandl E. S., Gorton M. P. (2002) Application of high field strength elements to discriminate tectonic settings in VMS environments. *Economic Geology* 97 (3): 629–642.

Sepahi A. A., Shahbazi H., Siebel W., Ranin A. (2014) Geochronology of plutonic rocks from the Sanandaj-Sirjan zone, Iran and new zircon and titanite U-Th-Pb ages for granitoids from the Marivan pluton. *Geochronometria* 41 (3): 207–215. DOI: https://doi.org/10.2478/s13386-013-0156-z.

Shabanian N., Davoudian A. R., Dong Y., Liu X. (2018) U-Pb zircon dating, geochemistry and Sr-Nd-Pb isotopic ratios from Azna-Dorud Cadomian metagranites, Sanandaj-Sirjan Zone of western Iran. *Precambrian Research* 306:41–60. DOI: https://doi.org/10.1016/j.precamres.2017.12.037.

Shabanian N., Khalili M., Davoudian A. R., Mohajjel M. (2009) Petrography and geochemistry of mylonitic granite from Ghaleh-Dezh, NW Azna, Sanandaj-Sirjan zone, Iran. *Neues Jahrbuch für Mineralogie-Abhandlungen. Journal of Mineralogy and Geochemistry* 185 (3): 233–248. DOI: https://doi.org/10.1127/0077-7757/2009/0121.

Shafaii Moghadam H., Li Q. L., Griffin W. L., Stern R. J., Ishizuka O., Henry H., Lucci F., O'Reilly S. Y., Ghorbani G. (2020) Repeated magmatic buildup and deep "hot zones" in continental evolution: the Cadomian crust of Iran. *Earth and Planetary Science Letters* 531 DOI: https://doi.org/10.1016/j.epsl.2019.11598.

Shahbazi H., Siebel W., Pourmoafee M., Ghorbani M., Sepahi A. A., Shang C. K., Vosoughi Abedini M. (2010) Geochemistry and U-Pb zircon geochronology of the Alvand plutonic complex in Sanandaj-Sirjan Zone (Iran): new evidence for Jurassic magmatism. *Journal of Asian Earth Sciences* 39 (6): 668–683. DOI: https://doi.org/10.1016/j.jseaes.2010.04.007.

Shahzeidi M., Moayyed M., Murata M., Yui T., Arai S., Chen F., Pirnia T., Ahmadian J. (2016) Late Ediacaran crustal thickening in Iran: Geochemical and isotopic constraints from the 550 Ma Mishu granitoids (northwest Iran). *International Geology Review* 59 (7): 793–811. DOI: https://doi.org/10.1080/00206814.2016.1198728.

Shellnutt J. G., Zhou M. F. (2007) Permian peralkaline, peraluminous and metaluminous A-type granites in the Panxi district, SW China: their relationship to the Emeishan mantle plume. *Chemical Geology* 243 (3–4): 286–316.

Sisson V. B., Pavlis T. L. (1993) Geologic consequences of plate reorganization: an example from the Eocene southern Alaska forearc. *Geology* 21 (10): 913–916.

Soesoo A. (2000) Fractional crystallization of mantle-derived melts as a mechanism for some I-type granite petrogenesis: an example from Lachlan Fold Belt, Australia. *Journal of the Geological Society* 157 (1): 135–149.

——— (1997) Mafic rocks associated with felsic intrusions—A key to understanding granite petrogenesis in SE Australia. *Geological Society of Australia* 46:27–28.

Stern R. (2023) Arc assembly and continental collision in the Neoproterozoic East African Orogen: implications for the consolidation of Gondwanaland. *Annual Review of Earth and Planetary Sciences* 22 (1): 319–351.

Stöcklin J. (1968) Structural history and tectonics of Iran: a review. *American Association of Petroleum Geologists Bulletin* 52 (7): 1229–1258.

Sun S. S., McDonough W. F. (1989) Chemical and isotopic systematics of oceanic basalts: implications for mantle composition and processes. *Geological Society, London, Special Publications* 42 (1): 313–345. DOI: https://doi.org/10.1144/GSL.SP.1989.042.01.19.

Tahmasebi Z., Castro A., Khalili M., Ahmadi Khalaji A., Rosa J. (2010) Petrologic and geochemical constraints on the origin of Astaneh pluton, Zagros orogenic belt, Iran. *Journal of Asian Earth Sciences* 39 (1–2): 81–96.

Tepper J. H., Nelson B. K., Bergantz G. W., Irving A. J. (1993) Petrology of the Chilliwack batholith, North Cascades, Washington: generation of calc-alkaline granitoids by melting of mafic lower crust with variable water fugacity. *Contributions to Mineralogy and Petrology* 113 (3): 333–351.

Thorkelson D. J. (1996) Subduction of diverging plates and the principles of slab window formation. *Tectonophysics* 255 (1–2): 47–63.

Torkian A., Khalili M., Sepahi A. A. (2008) Petrology and geochemistry of the I-type calc-alkaline Qorveh Granitoid Complex, Sanandaj-Sirjan Zone, western Iran. *Neues Jahrbuch für Mineralogie-Abhandlungen: Journal of Mineralogy and Geochemistry* 185 (2): 131–142. DOI: https://doi.org/10.1127/0077-7757/2008/0114.

Whalen J. B., Currie K. L., Chappell B. W. (1987) A-type granites — geochemical characteristics, discrimination and petrogenesis. *Contributions to Mineralogy and Petrology* 95 (4): 407–419.

Windley B. F., Xiao W. (2018) Ridge subduction and slab windows in the Central Asian Orogenic Belt: Tectonic implications for the evolution of an accretionary orogen. *Gondwana Research* 61:73–87. DOI: https://doi.org/10.1016/j.gr.2018.05.003.

Yanbo C., Jingwen M. (2010) Age and geochemistry of granites in Gejiu area, Yunnan province, SW China: constraints on their petrogenesis and tectonic setting. *Lithos* 120 (3–4): 258–276. DOI: https://doi.org/10.1016/j.lithos.2010.08.013.

Yang J. H., Wu F. Y., Wilde S. A., Chen F., Liu X. M., Xie L. W. (2008) Petrogenesis of an alkali Syenite-Granite-Rhyolite suite in the Yanshan Fold and Thrust Belt, Eastern North China Craton: Geochronological, geochemical and Nd-Sr-Hf isotopic evidence for lithospheric thinning. *Journal of Petrology* 49 (2): 315–351.

Yazdi A., ShahHoseini E., Razavi R. (2016) AMS, A method for determining magma flow in Dykes (Case study: Andesite Dyke). *Research Journal of Applied Sciences* 11 (3): 62–67. DOI: https://doi.org/10.3923/rjasci.2016.62.67.

Zhang Z., Xiao W., Ji W., Majidifard M. R., Rezaeian M., Talebian M., Xiang D., et al. (2018) Geochemistry, zircon U-Pb and Hf isotope for granitoids, NW Sanandaj-Sirjan zone, Iran: implications for Mesozoic Cenozoic episodic magmatism during Neo-Tethyan lithospheric subduction. *Gondwana Research* 62:227–245. DOI: https://doi.org/10.1016/j.gr.2018.04.002.

Zheng Y. F., Gong B., Zhao Z. F., Wu Y. B., Chen F. K. (2008) Zircon U-Pb age and O isotope evidence for Neoproterozoic low-δ^{18}O magmatism during supercontinental rifting in South China: Implications for the snowball Earth event. *American Journal of Science* 308 (4): 484–516.